



**Zurich University of Applied Sciences**

Department School of Engineering  
Institute of Computer Science

MASTER THESIS

---

**Tycho:**

**An Accuracy-First Architecture for Server-Wide  
Energy Measurement and Process-Level  
Attribution in Kubernetes**

---

*Author:*  
Caspar Wackerle

*Supervisors:*  
Prof. Dr. Thomas Bohnert  
Christof Marti

Submitted on  
January 31, 2026

Study program:  
Computer Science, M.Sc.

# Imprint

*Project:* Master Thesis  
*Title:* Tycho: An Accuracy-First Architecture for Server-Wide Energy Measurement and Process-Level Attribution in Kubernetes  
*Author:* Caspar Wackerle  
*Date:* January 31, 2026  
*Keywords:* process-level energy consumption, cloud, kubernetes  
*Copyright:* Zurich University of Applied Sciences

*Study program:*  
Computer Science, M.Sc.  
Zurich University of Applied Sciences

*Supervisor 1:*  
Prof. Dr. Thomas Bohnert  
Zurich University of Applied Sciences  
Email: thomas.michael.bohnert@zhaw.ch  
Web: [Link](#)

*Supervisor 2:*  
Christof Marti  
Zurich University of Applied Sciences  
Email: christof.marti@zhaw.ch  
Web: [Link](#)

# Abstract

## Abstract

The accompanying source code for this thesis, including all deployment and automation scripts, is available in the **PowerStack**[[1](#)] repository on GitHub.

# Contents

<b>Abstract</b>	<b>iii</b>
<b>1 Introduction</b>	<b>1</b>
1.1 Motivation . . . . .	1
1.2 Challenges and Limitations of Existing Approaches . . . . .	2
1.3 Problem Context . . . . .	2
1.4 Problem Statement . . . . .	2
1.5 Goals of This Thesis . . . . .	2
1.6 Research Questions . . . . .	2
1.7 Contributions . . . . .	2
1.8 Positioning Within Previous Work . . . . .	2
1.9 Scope and Boundaries . . . . .	3
1.10 Target Audience . . . . .	3
1.11 Origin of the Name “Tycho” . . . . .	3
1.12 Methodological Approach . . . . .	3
1.13 Ethical and Sustainability Considerations . . . . .	3
1.14 Thesis Structure . . . . .	3
1.15 System Environment for Development, Build and Debugging . . . . .	3
1.15.1 Host Environment and Assumptions . . . . .	3
1.15.2 Build Toolchain . . . . .	4
1.15.3 Debugging Environment . . . . .	4
1.15.4 Supporting Tools and Utilities . . . . .	5
1.15.5 Relevance and Limitations . . . . .	6
1.16 eBPF-collector-Based CPU Time Attribution . . . . .	6
1.16.1 Scope and Motivation . . . . .	6
1.16.2 Baseline and Architecture Overview . . . . .	7
1.16.3 Kernel Programs and Data Flow . . . . .	7
1.16.4 Collected Metrics . . . . .	8
1.16.5 Integration with Energy Measurements . . . . .	9
1.16.6 Efficiency and Robustness . . . . .	10
1.16.7 Limitations and Future Work . . . . .	10
1.17 GPU Collector Integration . . . . .	11
1.17.1 Introduction and Motivation . . . . .	11
1.17.2 Architectural Overview . . . . .	12
1.17.3 Phase-Aware Sampling: Conceptual Overview . . . . .	12
1.17.4 Phase-Aware Timing Model . . . . .	13
1.17.5 Event Lifecycle . . . . .	15
1.17.6 Per-Process Telemetry Window . . . . .	16
1.17.7 Collected Metrics . . . . .	17
1.17.8 Configuration Parameters . . . . .	18
1.17.9 Robustness and Limitations . . . . .	19
1.18 Redfish Collector Integration . . . . .	20
1.18.1 Overview and Objectives . . . . .	20
1.18.2 Baseline in Kepler . . . . .	20
1.18.3 Refactoring and Tycho Extensions . . . . .	21
1.18.4 Collected Metrics . . . . .	22
1.18.5 Integration and Data Flow . . . . .	23

1.18.6	Accuracy and Robustness Improvements . . . . .	23
1.18.7	Limitations . . . . .	24
1.19	Configuration Management . . . . .	24
1.19.1	Overview and Role in the Architecture . . . . .	24
1.19.2	Configuration Sources . . . . .	24
1.19.3	Implementation and Environment Variables . . . . .	24
1.19.4	Evolution in Newer Kepler Versions . . . . .	25
1.19.5	Available Parameters . . . . .	25
1.20	Timing Engine . . . . .	26
1.20.1	Overview and Motivation . . . . .	26
1.20.2	Architecture and Design . . . . .	26
1.20.3	Synchronization and Collector Integration . . . . .	27
1.20.4	Lifecycle and Configuration . . . . .	28
1.20.5	Discussion and Limitations . . . . .	28
1.21	Ring Buffer Implementation . . . . .	29
1.21.1	Overview . . . . .	29
1.21.2	Data Model and Sample Types . . . . .	29
1.21.3	Dynamic Sizing and Spare Capacity . . . . .	29
1.21.4	Thread Safety and Integration . . . . .	30
1.21.5	Idle Calibration . . . . .	30
1.21.6	Polling frequency Calibration . . . . .	30
1.21.7	Delay Calibration . . . . .	32
2	temporary notes on Pijnacker’s KUBEWATT	34
	Bibliography	50

## List of Figures

1.1	Phase-aware GPU polling timeline . . . . .	15
-----	--	----

## List of Tables

1.1	Metrics collected by the kernel eBPF subsystem. . . . .	9
1.2	Device- and MIG-level metrics collected by the GPU subsystem. . . . .	18
1.3	Process-level metrics collected over a backend-defined time window. .	18
1.4	Metrics collected by the Redfish collector. . . . .	23
1.5	User-facing configuration variables available in Tycho. . . . .	26

*The global climate crisis is one of humanity's greatest challenges in this century.  
With this work, I hope to contribute a small part in the direction we urgently need to go.*

## Chapter 1

# Introduction

### 1.1 Motivation

Global data center energy consumption is increasing rapidly, driven by the rising demand for compute-heavy workloads such as artificial intelligence and large-scale analytics. Data centers consumed roughly 1.5% of global electricity in 2024 (about 415 TWh) and are expected to more than double their consumption by 2030 [2]. At the same time, traditional sources of efficiency improvement, such as Moore’s law and Dennard scaling, are slowing down [3, 4], while gains from infrastructure optimizations approach diminishing returns [5, 6].

Containerized workloads form an increasingly large share of this growing footprint. They provide lightweight and scalable deployment mechanisms [7], and Kubernetes has become the dominant platform for orchestrating such workloads at scale. Despite their operational benefits and generally low overhead [8], containers make energy transparency difficult. Their shared-resource architecture and multi-layer abstraction obscure the relationship between individual workloads and the physical energy they consume, which complicates research on energy efficiency. As interest in energy-aware computing grows, accurate and fine-grained measurement becomes essential for research, performance engineering, and scheduling. Existing tools offer useful approximations but rely heavily on heuristic models and asynchronous telemetry, which limits their validity and reproducibility.

*Kepler*[9], a CNCF-backed project under active development, has become a widely adopted energy observability tool for Kubernetes clusters. Its design prioritizes portability, low overhead, and safe deployment across diverse environments, which makes it highly suitable for operational use at scale. A detailed analysis of its methodology and design philosophy is provided in Appendix A. In this context, Tycho is not intended to compete with Kepler or replace it. Instead, Tycho explores a complementary space: the upper bound of what measurement accuracy is achievable when higher-privilege monitoring methods, synchronized server-wide telemetry, and more fine-grained event-time alignment are permitted. While such techniques are often impractical for general-purpose deployments, they offer substantial value for research settings and large-scale R&D environments that require precise and reproducible energy measurements. Tycho is an attempt to fill this accuracy-focused niche by implementing methods that prioritize measurement fidelity over broad deployability.

## 1.2 Challenges and Limitations of Existing Approaches

Current approaches to workload-level energy estimation provide useful insights but remain limited in accuracy and reproducibility. Tools such as Kepler and Scaphandre[10] correlate resource utilization metrics with node-level energy telemetry, yet they operate under constraints that make fine-grained attribution difficult. Many systems depend on asynchronous and low-frequency sampling, rely on heterogeneous telemetry sources with differing clock domains, or employ heuristic models that introduce uncertainty. Purpose-built, high-accuracy measurement hardware exists, but its cost and operational overhead prevent widespread adoption in production environments. As a result, most available solutions offer high-level trends rather than precise, time-aligned measurements required for rigorous analysis. A more detailed discussion of these limitations is provided in § ?? and further expanded in Appendix A.

## 1.3 Problem Context

Modern container platforms such as Kubernetes run large numbers of heterogeneous, short-lived workloads on shared physical infrastructure. In multi-tenant clusters, containers continuously start, stop, migrate, and compete for CPU, memory, storage, and I/O resources. This dynamism complicates any attempt to determine how much energy a specific workload is responsible for.

At the hardware level, telemetry relevant to energy measurement is fragmented across multiple subsystems. Interfaces such as Intel RAPL, Redfish power sensors, GPU telemetry, and eBPF-based utilization metrics differ in sampling frequency, latency, and clock domain. Their values may arrive asynchronously and with inconsistent timing, making direct alignment difficult. Reliable attribution requires correlating these subsystems to a common time base, which existing platforms do not provide.

Kubernetes adds another layer of complexity. Processes are encapsulated inside containers, which in turn map to pods, cgroups, and namespaces that evolve over time. Accurate attribution therefore depends on robust tracking of process-to-container relationships and on resolving the timing mismatch between telemetry sources and the rapid state changes within the cluster. These combined factors make precise, container-level energy attribution a challenging problem.

## 1.4 Problem Statement

### 1.5 Goals of This Thesis

### 1.6 Research Questions

### 1.7 Contributions

### 1.8 Positioning Within Previous Work

This thesis builds directly on two earlier specialization projects completed as part of the Master’s program. The first project (VT1) focused on the practical deployment

of a bare-metal Kubernetes environment for energy efficiency research. It provided a fully automated setup procedure for cluster installation, persistent storage, monitoring infrastructure, and stress-test workloads, including all required configuration and connectivity. VT1 initially deployed Kepler as its energy monitoring component but has since been adapted to install Tycho instead, enabling rapid provisioning of complete measurement and evaluation environments. The resulting *PowerStack* repository [1] works in conjunction with this thesis by providing the operational foundation on which Tycho can be deployed and evaluated, and is documented in Appendix B.

The second project (VT2) examined the theoretical foundations of energy measurement in modern servers and containerized environments. It analyzed hardware-level telemetry interfaces, attribution challenges, and the strengths and limitations of existing tools, providing a structured overview of the state of the art. VT2 identified the methodological gaps that hinder precise workload-level energy attribution, many of which motivate the design choices in Tycho. A detailed version of this analysis is included in Appendix A.

The present thesis consolidates these two lines of work. It integrates the practical insights from VT1 with the theoretical findings of VT2 and develops Tycho as an accuracy-first system for server-wide energy measurement and workload attribution. In this role, the thesis serves as the point where the implementation, methodological foundations, and design philosophy come together into a coherent system.

## 1.9 Scope and Boundaries

### 1.10 Target Audience

### 1.11 Origin of the Name “Tycho”

### 1.12 Methodological Approach

### 1.13 Ethical and Sustainability Considerations

### 1.14 Thesis Structure

### 1.15 System Environment for Development, Build and Debugging

This section documents the environment used to develop, build, and debug *Tycho*; detailed guides live in [11].

#### 1.15.1 Host Environment and Assumptions

All development and debugging activities for *Tycho* were performed on bare-metal servers rather than virtualized instances. Development matched the evaluation target and preserved access to hardware telemetry such as RAPL, NVML, and BMC Redfish. The host environment consisted of Lenovo ThinkSystem SR530 servers (Xeon Bronze 3104, 64 GB DDR4, SSD+HDD, Redfish-capable BMC).

The systems ran Ubuntu 22.04 with a Linux 5.15 kernel. Full root access was available and required in order to access privileged interfaces such as eBPF. Kubernetes was installed directly on these servers using PowerStack[1], and served as the platform for deploying and testing *Tycho*. Access was via VPN and SSH within the university network.

### 1.15.2 Build Toolchain

Two complementary workflows are used: a dev path (local build, run directly on a node for interactive debugging) and a deploy path (build a container image, push to GHCR, deploy as a privileged DaemonSet via *PowerStack*).

#### 1.15.2.1 Local builds

The implementation language is Go, using `go version go1.25.1` on `linux/amd64`. The `Makefile` orchestrates routine tasks. The target `make build` compiles the exporter into `_output/bin/<os>_<arch>/kepler`. Targets for cross builds are available for `linux/amd64` and `linux/arm64`. The build injects version information at link time through `LDFLAGS` including the source version, the revision, the branch, and the build platform. This supports traceability when binaries or images are compared during experiments.

#### 1.15.2.2 Container images

Container builds use Docker Buildx with multi arch output for `linux/amd64` and `linux/arm64`. Images are pushed to the GitHub Container Registry under the project repository. For convenience there are targets that build a base image and optional variants that enable individual software components when required.

#### 1.15.2.3 Continuous integration

GitHub Actions produces deterministic images with an immutable commit-encoded tag, a time stamped dev tag, and a latest for `main`. Builds are triggered on pushes to the main branches and on demand. Buildx cache shortens builds without affecting reproducibility.

#### 1.15.2.4 Versioning and reproducibility

Development proceeds on feature branches with pull requests into `main`. Release images are produced automatically for commits on `main`. Development images are produced for commits on `dev` and for feature branches when needed. Dependency management uses Go modules with a populated `vendor/` directory. The files `go.mod` and `go.sum` pin the module versions, and `go mod vendor` materializes the dependency tree for offline builds.

### 1.15.3 Debugging Environment

The debugger used for *Tycho* is **Delve** in headless mode with a Debug Adapter Protocol listener. This provides a stable front end for interactive sessions while the debugged process runs on the target node. Delve was selected because it is purpose built for Go, supports remote attach, and integrates reliably with common editors without altering the build configuration beyond standard debug symbols.

### 1.15.3.1 Remote debugging setup

Debug sessions are executed on a Kubernetes worker node. The exporter binary is started under Delve in headless mode with a DAP listener on a dedicated TCP port. The workstation connects over an authenticated channel. In practice an SSH tunnel is used to forward the listener port from the node to the workstation. This keeps the debugger endpoint inaccessible from the wider network and avoids additional access controls on the cluster. To prevent metric interference the node used for debugging excludes the deployed DaemonSet, so only the debug instance is active on that host.

### 1.15.3.2 Integration with the editor

The editor is configured to attach through the Debug Adapter Protocol. In practice a minimal launch configuration points the adapter at the forwarded listener. Breakpoints, variable inspection, step control, and log capture work without special handling. No container specific extensions are required because the debugged process runs directly on the node.

The editor attaches over the SSH-forwarded DAP port; the inner loop is built locally with `make`, launch under Delve with a DAP listener, attach via SSH, inspect, adjust, repeat. When the goal is to validate behavior in a cluster setting rather than to step through code, the deploy oriented path is used instead. In that case the image is built and pushed, and observation relies on logs and metrics rather than an attached debugger.

### 1.15.3.3 Limitations and challenges

Headless remote debugging introduces some constraints. Interactive sessions depend on network reachability and an SSH tunnel, which adds a small amount of latency. The debugged process must retain the privileges needed for eBPF and access to hardware counters, which narrows the choice of where to run sessions on multi tenant systems. Running a second exporter in parallel on the same node would distort measurements, which is why the DaemonSet is excluded on the debug host. Container based debugging is possible but less convenient given the need to coordinate with cluster security policies. For these reasons, most active debugging uses a locally built binary that runs directly on the node, while container based deployments are reserved for integration tests and evaluation runs.

## 1.15.4 Supporting Tools and Utilities

### 1.15.4.1 Configuration and local orchestration

A lightweight configuration file `config.yaml` consolidates development toggles that influence local runs and selective deployment. Repository scripts read this file and translate high level options into concrete command line flags and environment variables for the exporter and for auxiliary processes. This keeps day to day operations consistent without editing manifests or code, and aligns with the two workflows in § 1.15.2. Repository scripts map configuration keys to explicit flags for local runs, debug sessions, and ad hoc deploys.

### 1.15.4.2 Container, cluster, and monitoring utilities

Supporting tools: Docker, kubectl, Helm, k3s, Rancher, Ansible, Prometheus, Grafana. Each is used only where it reduces friction, for example Docker for image builds, kubectl for interaction, and Prometheus/Grafana for observability.

## 1.15.5 Relevance and Limitations

### 1.15.5.1 Scope and contribution

The development, build, and debugging environment described in § 1.15.2 and § 1.15.3 is enabling infrastructure rather than a scientific contribution. Its purpose is to make modifications to *Tycho* feasible and to support evaluation, not to advance methodology in software engineering or tooling.

Documenting the environment serves reproducibility and auditability. A reader can verify that results were obtained on bare-metal with access to the required telemetry, and can reconstruct the build pipeline from source to binary and container image. The references to the repository at the start of this section in § 1.15 provide the operational detail that is intentionally omitted from the main text.

### 1.15.5.2 Boundaries and omissions

Installation steps, editor-specific configuration, system administration, security hardening, and multi tenant policy are out of scope; concrete commands live in the repository. Where concrete commands matter for reproducibility they are available in the repository documentation cited in § 1.15.

## 1.16 eBPF-collector-Based CPU Time Attribution

### 1.16.1 Scope and Motivation

The kernel-level eBPF subsystem in *Tycho* provides the foundation for process-level energy attribution. It captures CPU scheduling, interrupt, and performance-counter events directly inside the Linux kernel, translating them into continuous measurements of CPU ownership and activity. All higher-level aggregation and modeling occur in userspace; this section therefore focuses exclusively on the in-kernel instrumentation and the data it exposes.

Kepler's original eBPF design offered a coarse but functional basis for collecting CPU time and basic performance metrics. Its `sched_switch` tracepoint recorded process runtime, while hardware performance counters supplied instruction and cache data. However, the sampling cadence and aggregation logic were controlled from userspace, producing irregular collection intervals and temporal misalignment with energy readings. Kepler also treated all CPU time as a single undifferentiated category, omitting explicit representation of idle periods, interrupt handling, and kernel threads. As a result, a portion of the processor's activity (often significant under I/O-heavy workloads) remained unaccounted for in energy attribution.

*Tycho* addresses these limitations through a refined kernel-level design. New tracepoints capture hard and soft interrupts, while extended per-CPU state tracking distinguishes between user processes, kernel threads, and idle execution. Each CPU

maintains resettable bins that accumulate idle and interrupt durations within well-defined time windows, providing temporally bounded activity summaries aligned with energy sampling intervals. Cgroup identifiers are refreshed at every scheduling event to maintain accurate container attribution, even when processes migrate between control groups. The result is a stable, low-overhead data source that describes CPU usage continuously and with sufficient granularity to support fine-grained energy partitioning in the subsequent analysis.

### 1.16.2 Baseline and Architecture Overview

Kepler’s kernel instrumentation consisted of a compact set of eBPF programs that sampled process-level CPU activity and a few hardware performance metrics. The core tracepoint, `tp_btf/sched_switch`, captured context switches and estimated per-process runtime by measuring the on-CPU duration between successive events. Complementary probes monitored page cache access and writeback operations, providing coarse indicators of I/O intensity. Hardware performance counters (CPU cycles, instructions, and cache misses) were collected through `perf_event_array` readers, enabling approximate performance characterization at the task level.

While effective for general profiling, this setup lacked the temporal resolution and system coverage required for precise energy correlation. The sampling process was driven entirely from userspace, leading to irregular collection intervals, and idle or interrupt time was never observed directly. Consequently, CPU utilization appeared complete only from a process perspective, leaving kernel and idle phases invisible to the measurement pipeline.

Tycho extends this architecture into a continuous kernel-side monitoring system. Each CPU maintains an independent state structure recording its current task, timestamp, and execution context. This allows uninterrupted accounting of CPU ownership, even between user-space scheduling events. New tracepoints for hard and soft interrupts measure service durations directly in the kernel, ensuring that all processor activity (user, kernel, or idle) is captured. Dedicated per-CPU bins accumulate these times within fixed analysis windows, which the userspace collector periodically reads and resets. Process-level metrics are stored in an LRU hash map, while hardware performance counters remain integrated via existing PMU readers.

In contrast to Kepler’s snapshot-based sampling, Tycho’s userspace collector consolidates all per-process and per-CPU deltas from the kernel maps once per polling interval into a single tick. This tick-based aggregation provides deterministic timing, reduces memory pressure, and guarantees temporal consistency across heterogeneous metric sources. Data therefore flows linearly from tracepoints to per-CPU maps and onward to the collector, forming a continuous and low-overhead measurement path that supports precise, time-aligned energy attribution.

### 1.16.3 Kernel Programs and Data Flow

Tycho’s eBPF subsystem consists of a small set of tracepoints and helper maps that together maintain a continuous record of CPU activity. Each program updates per-CPU or per-task data structures in response to kernel events, ensuring that all processor time is accounted for across user, kernel, and idle contexts. The kernel side is event-driven and self-contained; aggregation into time-bounded ticks occurs later in userspace.

**Scheduler Switch** The central tracepoint, `tp_btf/sched_switch`, triggers whenever the scheduler replaces one task with another. It computes the elapsed on-CPU time of the outgoing process and updates its entry in the `processes` map, which stores cumulative runtime, hardware-counter deltas, and classification metadata such as `cgroup_id`, `is_kthread`, and command name. Hardware counters for instructions, cycles, and cache misses are read from preconfigured PMU readers at this moment, keeping utilization metrics temporally aligned with task execution. Each CPU also maintains a lightweight `cpu_state` structure that records the last timestamp, currently active PID, and task type. When the idle task (PID 0) is scheduled, this structure accumulates idle time locally, allowing continuous accounting even between user-space collection intervals. At polling time, the userspace collector drains these maps atomically, computing per-process deltas since the previous read and bundling all results into a single tick that represents the complete scheduler activity for that interval.

**Interrupt Handlers** To capture system activity outside user processes, Tycho introduces tracepoints for hard and soft interrupts. Pairs of entry and exit hooks (`irq_handler_entry,exit` and `softirq_entry,exit`) measure the time spent in each category by recording timestamps in the per-CPU state and adding the resulting deltas to dedicated counters. These durations are aggregated in `cpu_bins`, a resettable per-CPU array that also stores idle time. At each collection cycle, the userspace `bpfCollector` drains and resets these bins, incorporating their totals into the tick structure alongside the per-process deltas. This design maintains continuous coverage of kernel activity while preserving strict temporal alignment between CPU-state transitions and energy sampling.

**Page-Cache Probes** Kepler’s original page-cache hooks (`fexit/mark_page_accessed` and `tp/writeback_dirty_folio`) are preserved. They increment per-process counters for cache hits and writeback operations, serving as indicators of I/O intensity rather than direct power consumption. These counters are read and reset as part of the same tick aggregation that handles scheduler and interrupt data.

**Supporting Maps and Flow** All high-frequency updates occur in per-CPU or LRU hash maps to avoid contention. `pid_time_map` tracks start timestamps for active threads, enabling precise runtime computation during context switches. `processes` holds per-task aggregates, while `cpu_states` and `cpu_bins` manage temporal accounting per core. PMU event readers for cycles, instructions, and cache misses remain shared with Kepler’s implementation. At runtime, data flows from tracepoints to these maps and is drained periodically by the userspace collector, which consolidates the deltas into a single per-tick record before storing it in the ring buffer. This batched extraction forms a deterministic, lock-free telemetry path from kernel to analysis, ensuring high-frequency accuracy without per-event synchronization overhead.

#### 1.16.4 Collected Metrics

The kernel eBPF subsystem exports a defined set of metrics describing CPU usage at process and system levels. These values are aggregated in kernel maps and periodically retrieved by the userspace collector for time-aligned energy analysis. Table 1.1 summarizes all metrics grouped by category.

Metric	Source hook	Description
<i>Time-based metrics</i>		
Process runtime	<code>tp_btf/sched_switch</code>	Per process. Elapsed on-CPU time accumulated at context switches.
Idle time	Derived from <code>sched_switch</code>	Per CPU. Time with no runnable task (PID 0).
IRQ time	<code>irq_handler_{entry,exit}</code>	Per CPU. Duration spent in hardware interrupt handlers.
SoftIRQ time	<code>softirq_{entry,exit}</code>	Per CPU. Duration spent in deferred kernel work.
<i>Hardware-based metrics</i>		
CPU cycles	PMU ( <code>perf_event_array</code> )	Per process. Retired CPU cycle count during task execution.
Instructions	PMU ( <code>perf_event_array</code> )	Per process. Retired instruction count.
Cache misses	PMU ( <code>perf_event_array</code> )	Per process. Last-level cache misses; indicator of memory intensity.
<i>Classification and enrichment metrics</i>		
Cgroup ID	<code>sched_switch</code>	Per process. Control group identifier for container attribution.
Kernel thread flag	<code>sched_switch</code>	Per process. Marks kernel threads executing in system context.
Page cache hits	<code>mark_page_accessed</code>	Per process. Read or write access to cached pages; proxy for I/O activity.
IRQ vectors	<code>softirq_entry</code>	Per CPU. Frequency of specific soft interrupt vectors.

TABLE 1.1: Metrics collected by the kernel eBPF subsystem.

All metrics are aggregated once per polling interval into a single userspace tick that contains per-process and per-CPU deltas. This tick-based representation replaces the former per-sample storage model, ensuring temporal consistency across metrics while retaining the semantics listed above.

Together these metrics form a coherent description of CPU activity. Time-based data quantify ownership of processing resources, hardware counters capture execution intensity, and classification attributes link activity to its origin. This dataset serves as the kernel-level foundation for energy attribution and higher-level modeling in userspace.

### 1.16.5 Integration with Energy Measurements

The data exported from the kernel define how CPU resources are distributed among processes, kernel threads, interrupts, and idle periods during each observation window. When combined with energy readings obtained over the same interval, these temporal shares provide the basis for proportional energy partitioning. Instead of relying on statistical inference or coarse utilization averages, Tycho attributes energy according to directly measured CPU ownership.

Each collection tick consolidates all per-process runtime and performance-counter deltas together with per-CPU idle and interrupt bins. The sum of these components represents the total active time observed by the processor during that tick, matching the energy sample boundaries defined by the timing engine. This strict temporal alignment ensures that every joule of measured energy can be traced to a specific class of activity—user workload, kernel service, or idle baseline. Through this mechanism, the eBPF subsystem provides the precise temporal structure required for fine-grained, container-level energy attribution in the subsequent analysis stages.

### 1.16.6 Efficiency and Robustness

The kernel instrumentation is designed to operate continuously with negligible system impact while ensuring correctness across kernel versions. All high-frequency data reside in per-CPU maps, eliminating cross-core contention and locking. Each processor updates only its local entries in `cpu_states` and `cpu_bins`, while per-task data are stored in a bounded LRU hash that automatically removes inactive entries. Arithmetic within tracepoints is deliberately minimal (timestamp subtraction and counter increments only) so that the added latency per event remains near the measurement noise floor.

Userspace retrieval employs batched `BatchLookupAndDelete` operations, reducing system-call overhead and maintaining constant latency regardless of map size. Hardware counters are accessed through pre-opened `perf_event_array` readers managed by the kernel, avoiding repeated setup costs. Each polling interval consolidates the collected deltas into a single userspace tick, ensuring deterministic timing and consistent aggregation across all CPUs. This architecture allows the subsystem to record thousands of context switches per second while keeping CPU overhead low.

Correctness is maintained through several safeguards. CO-RE (Compile Once, Run Everywhere) field resolution protects the program from kernel-version differences in `task_struct` layouts. Cgroup identifiers are refreshed only for the newly scheduled task, ensuring accurate container labeling even when group membership changes. The idle task (PID 0) and kernel threads are handled explicitly to prevent user-space misattribution, and the resettable bin design enforces strict temporal separation between collection ticks. Together, these measures yield a stable and version-tolerant tracing layer that can run indefinitely without producing inconsistent or overlapping tick data.

### 1.16.7 Limitations and Future Work

Although the extended eBPF subsystem provides comprehensive temporal coverage of CPU activity, several limitations remain. Its precision is ultimately bounded by the granularity of available energy telemetry, as energy readings must be averaged over fixed collection intervals to remain stable. Within shorter ticks, power fluctuations introduce noise that limits the accuracy of direct attribution.

The current implementation also omits processor C-state and frequency information. While idle and active time are distinguished, variations in power state and dynamic frequency scaling are not yet represented in the collected data. Including tracepoints

such as `power:cpu_idle` and `power:cpu_frequency` would enable finer correlation between CPU state transitions and power usage. Additionally, very short-lived processes may terminate and be removed from the LRU map before the next tick is collected, leading to a slight underrepresentation of transient workloads.

## 1.17 GPU Collector Integration

### 1.17.1 Introduction and Motivation

Accelerators are increasingly responsible for the energy footprint of modern compute workloads. To attribute this consumption to containerized applications with high temporal accuracy, Tycho must incorporate GPU telemetry into the same unified timing model used for RAPL, eBPF, and Redfish domains (§ 1.20). Achieving this integration is challenging: GPU drivers do not expose continuous measurements but publish telemetry at discrete, hardware-dependent intervals. If these intervals are not respected, sampling quickly suffers from aliasing, redundant reads, and temporal drift across subsystems, as well as imprecise timing.

NVIDIA’s telemetry interfaces further complicate accurate measurement. The widely used `nvmlDeviceGetPowerUsage` function reports a *one-second trailing average*[12], not the instantaneous power required for sub-second energy attribution. High-frequency power samples are available only through specialised field APIs. Cumulative energy counters (when present) provide authoritative publish boundaries, but they are absent on many devices, including consumer GPUs and MIG configurations. Process-level telemetry is even more restrictive: NVML aggregates utilisation over caller-specified wall-clock windows and provides no information about the device’s internal publish cadence.

Because of these structural limitations, fixed polling intervals or naïve periodic sampling are fundamentally insufficient. Accurate attribution requires that Tycho (i) infer the GPU’s implicit publish cadence, (ii) align its sampling with this cadence, and (iii) integrate both device- and process-level telemetry into the global measurement timeline without violating the strict monotonic ordering enforced by Tycho’s multi-domain ring buffer (§ 1.21.1).

This work introduces two contributions that address these challenges:

- A **phase-aware sampling mechanism** that infers the GPU’s hidden publish rhythm and adaptively concentrates polling around predicted update edges. This transforms GPU sampling from periodic polling into a timing-aligned, event-driven process.
- A **unified integration of GPU telemetry** into Tycho’s global timebase, producing exactly one `GpuTick` per confirmed hardware update, with timestamps that are directly comparable to all other energy domains.

Together, these mechanisms provide temporally precise, low-latency GPU measurements while respecting the variability and constraints of NVIDIA’s telemetry ecosystem. This elevates the GPU subsystem to a first-class energy domain in Tycho and enables accurate container-level attribution in heterogeneous accelerator environments.

### 1.17.2 Architectural Overview

The GPU collector is organised as a layered subsystem that integrates vendor telemetry, adaptive timing, and unified buffering into a coherent measurement pipeline. Its structure reflects Tycho’s core design principles: strict adherence to a monotonic timebase, decoupling of heterogeneous sampling frequencies, and event-driven integration into the platform-wide timing and buffering infrastructure (§ 1.20, § 1.21.1).

At the lowest layer, the collector interfaces with NVIDIA accelerators through a backend abstraction compatible with both NVML and DCGM (“*Data Center GPU Manager*”). This abstraction handles device enumeration, capability probing, MIG topology inspection, and access to device and process telemetry. The collector does not assume uniform backend capabilities: cumulative energy counters, instantaneous power fields, and process-level utilisation may or may not be available depending on hardware generation and configuration.

Above this backend, the collector exposes two measurement paths:

- **Device path.** Retrieves power, utilisation, frequency, thermal, and memory metrics for all devices and MIG instances. These values describe the instantaneous operational state of the accelerator.
- **Process path.** Aggregates per-process utilisation over a backend-defined wall-clock window. This enables multi-tenant attribution but is inherently retrospective and independent of the device’s internal publish cadence.

Both paths feed into a shared sampling layer governed by Tycho’s timing engine. The device path is triggered by a *phase-aware scheduler* that aligns its polling activity with the driver’s implicit publish cadence. The process path is invoked only when a device update is detected, ensuring temporal alignment between instantaneous device measurements and aggregated process data.

The final integration step mirrors all other Tycho subsystems: each confirmed hardware update is converted into a `GpuTick` structure containing device and (optionally) process snapshots, together with a strictly ordered monotonic timestamp. This tick is emitted into Tycho’s multi-domain ring buffer, where it becomes part of the unified energy timeline used for correlation and attribution across eBPF, RAPL, and platform power domains.

Figure 1.1 (later in this section) provides a conceptual overview of this pipeline, illustrating the interaction between the backend interface, the phase-aware sampler, and Tycho’s global collection engine.

### 1.17.3 Phase-Aware Sampling: Conceptual Overview

GPU drivers publish power and utilisation metrics at discrete, device-internal intervals. These updates occur neither continuously nor synchronously with the sampling frequencies required by Tycho’s timing engine. Because the driver does not expose its publish cadence directly, a naïve fixed-interval polling strategy risks both *aliasing* (missing updates) and *redundancy* (repeatedly reading identical values). Either effect would distort the temporal alignment of GPU measurements with the rest of Tycho’s energy domains.

To avoid this, the GPU collector introduces a *phase-aware sampling* mechanism that infers the driver’s implicit publish cadence from observations. The sampler tracks two quantities: an estimated publish period and the phase offset between the device’s update rhythm and Tycho’s monotonic timebase. By predicting the next likely update moment, the sampler can modulate its polling intensity accordingly:

- **Base mode:** low-frequency polling maintains coarse alignment and detects long-term drift in the publish cadence.
- **Burst mode:** when the current time approaches a predicted update edge, the sampler briefly increases its polling frequency to minimise the latency between the hardware update and Tycho’s observation of it.

This adaptive strategy ensures that Tycho reads the device only when a fresh publish is likely to be available. Freshness is determined by comparing each snapshot to the most recent confirmed update, preferably via cumulative energy counters when present, or otherwise via power deltas exceeding a configurable threshold. Only when a new publish is detected does the sampler emit an event.

The resulting behaviour is simple but powerful:

*Each hardware update produces exactly one `GpuTick`, and no tick is emitted unless the device has genuinely updated.*

This one-to-one correspondence is critical for integrating GPU measurements into Tycho’s unified energy timeline. It guarantees temporal fidelity, eliminates redundant samples, and ensures that GPU metrics are directly comparable with other measurements obtained under the same timing and buffering semantics.

The next subsection formalises this behaviour by presenting the timing model used to estimate publish periods, track phase offsets, and define the burst window around predicted update edges.

#### 1.17.4 Phase-Aware Timing Model

The timing model enables Tycho to infer the GPU driver’s implicit publish cadence and to align sampling with the actual update moments of the hardware. It maintains two quantities derived from confirmed device updates: an estimate of the *publish period* and a *phase offset* relative to Tycho’s monotonic clock. This subsection presents the model in a unified mathematical form.

Let  $t_{\text{obs},k}$  denote the monotonic timestamp of the  $k$ -th confirmed hardware update. From these observations, the sampler derives the period estimate  $\hat{T}_k$  and phase estimate  $\hat{\phi}_k$ .

**Period Estimation.** Each new inter-update interval

$$\Delta t_k = t_{\text{obs},k} - t_{\text{obs},k-1}$$

provides a direct sample of the device’s publish period. To remain robust to jitter caused by DVFS, thermal transitions, or backend noise, the sampler applies an exponential moving average (EMA):

$$\hat{T}_k = (1 - \alpha_T) \hat{T}_{k-1} + \alpha_T \Delta t_k,$$

with  $\alpha_T \in (0, 1)$  controlling the smoothing strength. The resulting estimate is clamped to a stable range derived from Tycho’s engine cadence, ensuring predictable behaviour across different GPUs.

**Phase Tracking.** Given a current period estimate, the expected time of the  $k$ -th update is

$$\hat{t}_k = t_{\text{obs},k-1} + \hat{\phi}_{k-1} + \hat{T}_k.$$

The deviation

$$\delta_k = t_{\text{obs},k} - \hat{t}_k$$

represents the phase error. The sampler updates its phase estimate through a second EMA:

$$\hat{\phi}_k = (\hat{\phi}_{k-1} + \alpha_\phi \delta_k) \bmod \hat{T}_k,$$

where  $\alpha_\phi$  is a small adaptation constant. This ensures smooth convergence toward the device’s true publish rhythm.

**Edge Prediction.** At an arbitrary time  $t_{\text{now}}$ , the predicted next update edge is

$$t_{\text{next}} = t_{\text{obs},k} + n \cdot \hat{T}_{k+1} + \hat{\phi}_{k+1},$$

where  $n$  is the smallest non-negative integer such that  $t_{\text{next}} \geq t_{\text{now}}$ . This prediction determines where sampling effort should be concentrated.

**Burst Window.** To avoid continuous high-frequency polling, the sampler restricts hyperpolling to a narrow window of half-width  $w$  around  $t_{\text{next}}$ :

$$\text{mode}(t_{\text{now}}) = \begin{cases} \text{burst}, & |t_{\text{now}} - t_{\text{next}}| \leq w, \\ \text{base}, & \text{otherwise.} \end{cases}$$

The width  $w$  is expressed as a fraction of the calibrated engine cadence, ensuring proportional behaviour across platforms.

**Summary.** The phase-aware model enables Tycho to infer the GPU’s implicit publish cadence solely from observed updates and to align sampling with the device’s true update edges. By combining smooth period estimation, adaptive phase correction, and narrow burst windows around predicted publishes, the sampler detects new hardware updates with low latency and emits exactly one `GpuTick` per publish.

Figure 1.1 visualises the behaviour of the phase-aware sampling model introduced above. The top lane represents the hardware’s implicit publish sequence; the middle lane shows Tycho’s adaptive polling pattern during both calibration and the phase-locked regime; and the bottom lane shows the resulting GPU ticks, demonstrating the one-to-one mapping between fresh device updates and emitted `GpuTick` events.

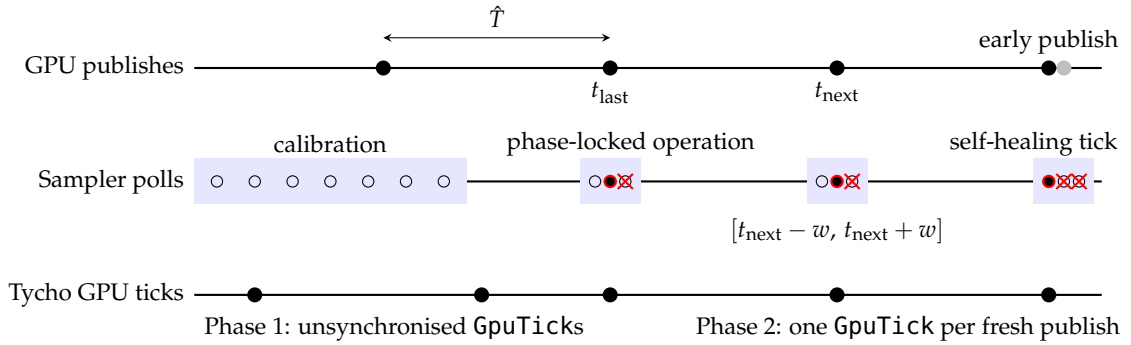


FIGURE 1.1: Phase-aware GPU polling timeline

### 1.17.5 Event Lifecycle

The GPU collector converts each confirmed hardware update into a monotonically-timestamped **GpuTick** that integrates into Tycho’s multi-domain energy timeline. The lifecycle consists of five stages: polling, device acquisition, optional process acquisition, freshness detection, and tick emission.

**1. Poll Initiation.** Polling is triggered solely by the phase-aware scheduler (§ 1.17.3, § 1.17.4). Base-mode polls track long-term cadence drift; burst-mode polls densely probe the vicinity of predicted update edges. Each poll receives a monotonic timestamp  $t_{\text{now}}$  that anchors the resulting event.

**2. Device Snapshot Acquisition.** A poll retrieves device-level telemetry for all GPUs and MIG instances, capturing power, utilisation, clocks, thermals, and memory state. All values reflect the device’s instantaneous condition at  $t_{\text{now}}$  and form a consistent cross-device snapshot of the accelerator subsystem.

**3. Optional Process Snapshot Acquisition.** If available, process-level telemetry is sampled over a backend-defined wall-clock window (§ 1.17.6). Although retrospective, these samples are associated with the same monotonic timestamp as the device snapshot, ensuring that device and process data remain correlated without temporal ambiguity.

**4. Freshness Determination.** The collector compares the new device snapshot with the most recent confirmed update. Cumulative energy counters, when available, serve as the authoritative freshness signal; otherwise Tycho uses a power-delta threshold to avoid counting noise as updates. Only fresh snapshots update the period and phase estimators and proceed to the next stage.

**5. Tick Emission.** A fresh observation is converted into a **GpuTick** containing device and (optional) process snapshots and the timestamp  $t_{\text{now}}$ . The tick is then delivered to Tycho’s multi-domain ring buffer (§ 1.21.1). If no fresh update is detected, the poll produces no tick, ensuring that the GPU timeline faithfully reflects the hardware’s publish cadence.

**Summary.** The event lifecycle ensures that GPU telemetry is sampled only when meaningful, timestamped consistently with Tycho’s timebase, and integrated without blocking or duplication. Each hardware update generates exactly one `GpuTick`, providing a precise, causally ordered input to Tycho’s cross-domain energy attribution pipeline.

### 1.17.6 Per-Process Telemetry Window

Device-level metrics describe the instantaneous state of each GPU, but many applications require attributing accelerator activity to individual processes or containers. NVIDIA’s interfaces provide such information only in the form of *aggregated utilisation over a caller-specified time window*. Correctly selecting and interpreting this window is essential for obtaining meaningful per-process data and for aligning process-level records with the device-level timeline maintained by Tycho.

**Wall-Clock Semantics.** Unlike device publishes, which occur on the GPU’s internal cadence, NVIDIA’s per-process APIs integrate utilisation over a duration supplied by the caller. These interfaces expect a *wall-clock* interval, expressed in milliseconds, rather than a duration derived from Tycho’s monotonic timebase. The distinction is crucial: Tycho’s monotonic clock operates on an internal quantum chosen to support high-resolution scheduling (§ 1.20), but this quantum has no defined relationship to real elapsed time. Using monotonic differences directly would produce windows that are several orders of magnitude too short, yielding incomplete utilisation samples.

For this reason, Tycho maintains a separate wall-clock origin for each GPU or MIG instance. Whenever process telemetry is requested, the duration since the last successful query is computed using wall-clock time, ensuring that the backend receives a true real-time interval.

**Window Derivation.** For each owner (physical GPU or MIG instance), Tycho records the timestamp  $t_{\text{last}}^{(i)}$  of the most recent successful process query. When a new query occurs at time  $t_{\text{now}}^{(i)}$ , the raw duration

$$\Delta t_{\text{raw}}^{(i)} = t_{\text{now}}^{(i)} - t_{\text{last}}^{(i)}$$

is transformed according to backend expectations:

1. *Clamping*. The duration is restricted to a safe range  $\Delta t_{\min} \leq \Delta t^{(i)} \leq \Delta t_{\max}$  to avoid zero-length or excessively long sampling windows.
2. *Millisecond granularity*. NVIDIA’s process APIs accept durations in whole milliseconds. Tycho therefore rounds the clamped value up to the next full millisecond to prevent systematic underestimation of utilisation.

After a successful query, the wall-clock origin is updated to  $t_{\text{last}}^{(i)} \leftarrow t_{\text{now}}^{(i)}$ , establishing continuity across successive sampling windows.

**Temporal Alignment with Device Updates.** Even though per-process telemetry describes accumulated activity rather than a snapshot, Tycho ensures that all process samples remain aligned with the device timeline. Each process record is associated

with the device-level timestamp of the poll that triggered the query. If a device has never produced a fresh update, the collector uses the timestamp of the most recent device tick as the initial origin for its process window. This guarantees that device and process metrics are linked to the same global temporal reference and can be fused without interpolation.

**Backend Variability and Robustness.** Process-level support varies widely across NVIDIA hardware and software stacks. DCGM-capable systems typically expose high-quality, high-resolution utilisation data, whereas NVML-only systems (particularly consumer GPUs) may provide limited or noisy information. Tycho’s design accommodates these differences gracefully: when a process query fails, the wall-clock origin is still advanced to prevent tight retry loops, and device-level sampling proceeds unaffected. This ensures stable behaviour even in mixed configurations where only a subset of devices expose meaningful per-process telemetry.

**Summary.** By separating wall-clock process windows from monotonic device timestamps and carefully aligning both within Tycho’s timing architecture, the GPU collector provides process-level telemetry that is semantically correct, temporally consistent, and robust to backend limitations. This separation of concerns is essential for accurate multi-tenant attribution in heterogeneous accelerator environments.

### 1.17.7 Collected Metrics

The GPU collector reports two complementary categories of telemetry that together describe both the instantaneous state of each accelerator and the distribution of GPU activity across processes. All metrics are incorporated into a unified `GpuTick` structure and timestamped under Tycho’s monotonic timebase, ensuring direct comparability with other domains.

**Device-Level Metrics.** Device and MIG-level metrics capture the operational state of the accelerator at the moment Tycho detects a fresh hardware update. These values include power, utilisation, memory usage, thermal data, and clock frequencies, along with backend-specific fields such as instantaneous power samples or cumulative energy counters. Cumulative energy, when available, is used as the authoritative indicator of publish boundaries and therefore plays a central role in the timing model and freshness detection. Due to a tendency of NVIDIA GPUs to still produce (invalid) values when queried for cumulative energy, the actual availability of correct cumulative energy-metrics is verified during the initial calibration.

**Process-Level Metrics.** Process-level metrics describe the aggregated utilisation of individual processes over the backend-defined wall-clock window (§ 1.17.6). They enable multi-tenant attribution by associating GPU activity with specific applications, containers, or pods. Because these values represent accumulated work rather than an instantaneous snapshot, they are paired with the device-level timestamp of the triggering poll, ensuring temporal consistency within Tycho’s unified timeline.

Tables 1.2 and 1.3 summarise the metrics collected at both levels.

Metric	Unit	Description
<i>Utilisation metrics</i>		
SMUtilPct	%	Streaming multiprocessor (SM) utilisation.
MemUtilPct	%	Memory controller utilisation.
EncUtilPct	%	Hardware video encoder utilisation.
DecUtilPct	%	Hardware video decoder utilisation.
<i>Energy and thermal metrics</i>		
PowerMilliW	mW	Instantaneous power via NVML/DCGM (1s average).
InstantPowerMilliW	mW	High-frequency instantaneous power from NVIDIA field APIs.
CumEnergyMilliJ	mJ	Cumulative energy counter (preferred freshness signal).
TempC	°C	GPU temperature.
<i>Memory and frequency metrics</i>		
MemUsedBytes	bytes	Allocated framebuffer memory.
MemTotalBytes	bytes	Total framebuffer memory.
SMClockMHz	MHz	SM clock frequency.
MemClockMHz	MHz	Memory clock frequency.
<i>Topology and metadata</i>		
DeviceIndex	–	Numeric device identifier.
UUID	–	Stable device UUID.
PCIBusID	–	PCI bus identifier.
IsMIG	–	Indicates a MIG instance.
MIGParentID	–	Parent device index for MIG instances.
Backend	–	Backend type (NVML or DCGM).

TABLE 1.2: Device- and MIG-level metrics collected by the GPU subsystem.

Metric	Unit	Description
Pid	–	Process identifier.
ComputeUtil	%	Per-process SM utilisation aggregated over the query window.
MemUtil	%	Per-process memory controller utilisation.
EncUtil	%	Per-process encoder utilisation.
DecUtil	%	Per-process decoder utilisation.
GpuIndex	–	Device or MIG instance to which the sample belongs.
GpuUUID	–	Corresponding device UUID.
TimeStampUS	µs	Backend timestamp associated with the utilisation record.
<i>MIG metadata (when applicable)</i>		
GpuInstanceID	–	MIG GPU instance identifier.
ComputeInstanceID	–	MIG compute-instance identifier.

TABLE 1.3: Process-level metrics collected over a backend-defined time window.

### 1.17.8 Configuration Parameters

The GPU collector exposes only a minimal set of configuration parameters. In contrast to traditional monitoring systems that require hand-tuned polling intervals, Tycho derives the parameters of the phase-aware sampler directly from the engine cadence calibrated during system startup (§ 1.20). This ensures that GPU sampling

inherits the same temporal consistency as all other energy domains and remains robust across heterogeneous hardware.

The configuration governs three tightly coupled aspects of the sampling mechanism:

- **Cadence bounds.** The initial estimate of the GPU publish period, as well as its minimum and maximum permissible values, are expressed as simple fractions of the engine cadence. This constrains the period estimator to a stable range without relying on device-specific heuristics.
- **Polling intervals.** Both base-mode and burst-mode polling frequencies are derived from fixed ratios of the engine cadence. As a result, Tycho polls aggressively only when a publish is predicted without requiring manual tuning.
- **Burst-window width.** The half-width of the burst window around  $t_{\text{next}}$  is likewise tied to the engine cadence. This determines how narrowly the sampler focuses its hyperpolling effort around predicted publish edges.

Because all parameters scale with the calibrated cadence, the sampler adapts automatically to different GPU generations, backend behaviours, and platform timing characteristics. No user-facing configuration is required; temporal correctness follows directly from Tycho’s system-wide timing model.

### 1.17.9 Robustness and Limitations

The GPU collector is designed to operate reliably across heterogeneous hardware, backend capabilities, and driver behaviours. Its phase-aware sampling, decoupled event queue, and unified timebase ensure that GPU telemetry integrates cleanly with Tycho’s multi-domain measurement framework. Nevertheless, several structural constraints in NVIDIA’s telemetry ecosystem define the practical limits of what can be inferred and with what temporal precision.

**Backend Variability.** The capabilities of NVML and DCGM differ significantly across GPU generations and product classes. Datacenter GPUs typically expose cumulative energy counters, high-frequency instant power fields, and stable process-level utilisation, while consumer GPUs often lack cumulative energy and provide only coarse utilisation metrics. Tycho handles these differences gracefully (sampling continues even when certain fields are missing) but the quality of the resulting attribution reflects the capabilities of the underlying hardware.

**Power Measurement Limitations.** The widely used `nvmlDeviceGetPowerUsage` call provides a *one-second trailing average*, which is unsuitable as a high-frequency power signal. Tycho therefore relies on instantaneous power fields (e.g. field 186) when available, and uses cumulative energy counters as the authoritative freshness indicator. On devices lacking both instantaneous fields and cumulative energy, power-based freshness detection becomes less precise, increasing uncertainty in the inferred publish cadence.

**Process Attribution Constraints.** Process-level utilisation is inherently aggregated over a wall-clock window, since NVIDIA provides no access to per-process instantaneous state. This retrospective design imposes two limitations: (i) spikes shorter

than the sampling window may be attenuated, and (ii) per-process values cannot be aligned to the exact moment of a device publish. Tycho addresses this by using the device-level timestamp to anchor all process records, but the granularity of attribution ultimately depends on backend resolution.

**Cadence Inference and Jitter.** Because the driver does not expose its publish cadence, Tycho must infer it indirectly. Under conditions of high load, thermal transitions, or DVFS-induced jitter, publish intervals may vary, introducing uncertainty into edge prediction. Tycho’s EMA-based estimators maintain stability under such variability, but prediction accuracy is inherently bounded by the noisiness of the underlying telemetry.

**Mixed and MIG Configurations.** Systems combining MIG and non-MIG devices, or devices with partial telemetry support, may expose inconsistent field availability across accelerators. Cumulative energy counters may exist for some instances but not others; process information may be available only at the parent-device level. Tycho handles these cases through per-device fallbacks and independent cadence models, but the precision of multi-GPU attribution varies with the fidelity of each device’s telemetry.

**Vendor support scope.** The current GPU collector supports only NVIDIA-based accelerators, following the design of Kepler. While this excludes other vendors, it is justifiable: according to market research[13], NVIDIA captured approximately 93% of the server GPU revenue in 2024. Given this dominant share, focusing on NVIDIA hardware is acceptable for the majority of data-centre GPU deployments.

## 1.18 Redfish Collector Integration

The Redfish collector retrieves node-level power data from the server’s Baseboard Management Controller (BMC) via the Redfish API. As an out-of-band source, it complements in-band interfaces such as RAPL by providing an external, hardware-validated view of total system power. Tycho integrates this telemetry into its synchronized measurement framework, ensuring consistent timing and comparability across collectors.

### 1.18.1 Overview and Objectives

Redfish power metrics are vendor-defined and updated asynchronously, with variable latency and precision. The Tycho implementation therefore focuses on reliability, timing control, and consistent timestamping. All polling, freshness tracking, and temporal alignment are managed centrally by Tycho, allowing Redfish samples to be merged with other data sources for later workload-level energy attribution.

### 1.18.2 Baseline in Kepler

In Kepler, the Redfish implementation provided a minimal wrapper around the BMC’s `/redfish/v1/Chassis/*/Power` endpoint. Its sole purpose was to retrieve aggregated chassis power at a fixed interval and expose it through the node-level energy interface used by the power model. The default polling frequency was

set to 60 seconds, adequate for coarse monitoring but too infrequent for detailed analysis.

At such long intervals, issues like repeated values or timing drift were largely masked by the coarse sampling period. However, the design offered no mechanisms to detect new versus stale data, to associate samples with BMC timestamps, or to align readings precisely with other metrics. The internal background ticker operated independently of other Kepler collectors, providing no unified notion of time or freshness. Kepler’s Redfish integration was therefore sufficient for low-resolution system energy reporting, but not designed for higher measurement intervals or fine-grained temporal correlation.

### 1.18.3 Refactoring and Tycho Extensions

#### 1.18.3.1 Timing Ownership and Polling Control

Tycho removes Kepler’s internal ticker and delegates all Redfish polling to its centralized timing engine. To account for the unpredictable nature of BMC update cycles, Tycho introduces an optional adaptive mode governed by `TYCHO_REDIFISH_POLL_AUTOTUNE`. When enabled, the collector dynamically infers a suitable polling interval from observed publication gaps, learning the effective refresh frequency of the specific Redfish implementation. When disabled, Tycho performs fixed-interval polling strictly at the user-defined cadence, preserving deterministic operation.

By externalizing timing control, the collector decouples sampling from Redfish’s internal pacing, enabling reproducible experiments and consistent temporal correlation with other measurement sources.

#### 1.18.3.2 Header-Based Newness and Sequence Tracking

When polled at higher frequencies, Redfish endpoints often repeat identical payloads until the BMC updates its internal sensors. To avoid redundant samples, Tycho introduces a lightweight newness detection mechanism combining HTTP headers and value comparison.

Each response is inspected for the `ETag` and `Date` headers. If an `ETag` differs from the previously stored value, or if the `Date` timestamp is newer, the sample is treated as fresh. If no header change is observed, Tycho falls back to value-based detection by comparing the reported power against the previous reading. A monotonically increasing `seq` counter is maintained per chassis to mark every distinct update, allowing downstream components to identify repeated or skipped readings unambiguously.

This design provides consistent differentiation between new and stale measurements without requiring vendor-specific heuristics. It also ensures that timestamp alignment and freshness analysis remain reliable even when Redfish responses arrive irregularly or contain repeated values.

#### 1.18.3.3 Heartbeat Mechanism and Freshness Metric

Because Redfish publication intervals can vary considerably between BMC implementations, Tycho introduces a heartbeat mechanism to ensure continuous sample availability. If no new data are received within a configurable timeout, defined by

TYCHO\_REDISH\_HEARTBEAT\_MAX\_GAP\_MS, the collector emits a heartbeat sample that reuses the last known power value. This prevents temporal gaps in the time series and maintains a consistent data flow for later energy integration.

Each emitted sample also carries a *freshness* metric, representing the time difference between the Redfish-reported Date header (if present) and the local collection timestamp. This value quantifies the staleness of a reading and allows the analysis layer to account for delayed or buffered updates. In practice, freshness remains below one second on well-behaved BMCs but can increase significantly under heavy load or poor firmware timing.

Together, the heartbeat and freshness metric allow Tycho to stabilize asynchronous Redfish data streams and provide temporal confidence estimates for each sample.

#### 1.18.3.4 Fixed vs Auto Polling Mode

Tycho supports two complementary Redfish polling strategies, selectable via TYCHO\_REDISH\_POLL\_AUTOTUNE. In *fixed mode* (`false`), polling occurs strictly at the user-defined cadence TYCHO\_REDISH\_POLL\_MS. This mode guarantees deterministic timing and is suited for controlled experiments where Redfish irregularities are tolerable or where timing synchronization with other collectors is critical.

When *auto mode* (`true`) is enabled, the collector dynamically adjusts its internal expectations to match the observed publication rhythm of the BMC. It derives the median inter-arrival time of new Redfish samples and adapts the expected heartbeat gap accordingly. This allows the collector to align its emission behavior with the actual update frequency of the hardware, minimizing redundant polls and improving temporal coherence between samples.

XX

THIS SECTION NEEDS TO BE UPDATED UPON CALIBRATION PACKAGE COMPLETION

A future calibration module will further refine POLL\_MS and related delay parameters based on startup profiling, but this mechanism remains outside the collector itself. Within Tycho, the auto mode provides a self-stabilizing behavior that balances responsiveness with measurement overhead, while the fixed mode ensures reproducibility for benchmark-oriented studies. XXXXXXXXXXXXXXXXXXXXXXXXXXXXXXX

#### 1.18.4 Collected Metrics

The Redfish collector retrieves instantaneous power readings from the BMC for each physical chassis. Unlike software-based collectors, it provides direct hardware telemetry at node level and does not expose component-level breakdowns. All readings are timestamped, aligned to Tycho's global monotonic clock, and supplemented with freshness and sequence metadata to support temporal correlation. Table 1.4 lists the collected fields.

These metrics provide a coherent node-level view of power consumption with explicit temporal context, forming the hardware baseline for higher-level attribution in later stages of the Tycho pipeline.

Metric	Unit	Description
<i>Primary power metrics</i>		
PowerWatts	W	Instantaneous chassis power draw reported by the BMC via <code>/redfish/v1/Chassis/*/Power</code> .
<i>Temporal and identity metadata</i>		
EnergyMilliJ	mJ	Integrated node energy derived from consecutive power samples (computed downstream).
<i>Operational context</i>		
ChassisID	-	Identifier of the chassis or enclosure corresponding to the Redfish endpoint.
Seq	-	Incremental counter marking each new reading as determined by header or value changes.
SourceTime	s	Original BMC timestamp parsed from the HTTP Date header, if available.
CollectorTime	s	Local collection time according to Tycho's monotonic clock.
FreshnessMs	ms	Time difference between SourceTime and CollectorTime, indicating sample latency.
Heartbeat	flag	Marks a repeated emission when no new BMC data were available within the configured heartbeat interval.
PollMode	enum	Indicates whether fixed or auto polling mode was active during sampling.

TABLE 1.4: Metrics collected by the Redfish collector.

### 1.18.5 Integration and Data Flow

The Redfish collector operates as a passive data source within Tycho's unified collection framework. It queries the BMC through the Redfish API, extracts instantaneous chassis power, and writes each result into a synchronized ring buffer shared with the central engine. Each record carries both system- and collection-time metadata, enabling later temporal alignment during analysis.

This integration layer is deliberately lightweight: the collector's responsibility ends once valid samples are obtained and buffered. All subsequent processing is handled by Tycho's analysis modules. This separation keeps the collector simple, minimizes coupling to higher layers, and isolates potential BMC irregularities from the rest of the system.

### 1.18.6 Accuracy and Robustness Improvements

Tycho introduces several measures to improve the precision and reliability of Redfish telemetry compared to Kepler. Header-based newness detection ensures that only genuinely updated readings are processed, reducing redundant samples caused by repeated BMC responses. Each reading carries a freshness metric that quantifies its temporal distance from the BMC's internal timestamp, providing explicit visibility into data latency. A lightweight heartbeat mechanism compensates for occasional gaps or stalls in BMC reporting, maintaining continuity in the power time

series without fabricating new information.

These measures collectively enhance stability across heterogeneous Redfish implementations and ensure that all retained samples are both valid and chronologically consistent.

### 1.18.7 Limitations

Despite its improved design, the Redfish collector remains constrained by the capabilities and responsiveness of the underlying BMC. Sampling frequency is typically limited to one or two seconds, and the precision of reported timestamps varies widely across vendors. No component-level breakdown is available (only total chassis power), restricting fine-grained attribution to software-based collectors such as RAPL or eBPF.

## 1.19 Configuration Management

### 1.19.1 Overview and Role in the Architecture

Tycho adopts a simple, centralized configuration layer that is initialized during exporter startup and made globally accessible through typed structures. This layer defines all runtime parameters controlling timing, collection, and analysis behaviour. It serves as the interface between user-defined settings and the internal scheduling and buffering logic described in § 1.20.

The configuration is loaded once at startup, combining defaults, environment variables, and optional overrides passed through Helm or local flags. Its purpose is not to support dynamic reconfiguration, but to provide deterministic, reproducible operation across (experimental) runs. No backward compatibility with previous Kepler versions is maintained.

### 1.19.2 Configuration Sources

Configuration values can be provided in three ways: first, through a `values.yml` file during Helm installation, second, as command-line flags for local or debugging builds, and third, via predefined environment variables that act as defaults.

During startup, Tycho sequentially evaluates these sources in fixed order—defaults are loaded first, then environment variables, followed by any user-supplied overrides. The resulting configuration is stored in memory and printed once for verification. After initialization, all components reference the same in-memory configuration, ensuring consistent behaviour across collectors and analysis modules.

### 1.19.3 Implementation and Environment Variables

The configuration implementation in Tycho closely follows the approach used in Kepler v0.9.0. Each configuration key is mapped to an environment variable, which is resolved at startup through dedicated lookup functions. If no variable is set, the corresponding default value is applied. This mechanism enables flexible configuration without external dependencies or complex parsing logic. All variables are read once during initialization, after which they are cached in typed configuration structures. This guarantees consistent operation even if environment variables change

later, since Tycho is not designed for live reconfiguration. The configuration layer is invoked before the collectors and timing engine are instantiated, ensuring that parameters such as polling intervals, buffer sizes, or analysis triggers are available to all components from the first cycle onward.

#### 1.19.3.1 Validation and Normalization at Startup

During initialization, Tycho validates all user inputs and normalizes them to a consistent, safe configuration. First, basic bounds are enforced: the global timebase quantum must be positive, non-negative values are required for all periods and delays, and missing essentials fall back to minimal defaults. Trigger coherence is then checked. If `redfish` is selected while the Redfish collector is disabled, Tycho switches to the timer trigger and ensures a valid interval. Unknown triggers default to `timer`.

All periods and delays are aligned to the global quantum so that scheduling, buffering, and analysis operate on a common time grid. The analysis wait `DelayAfterMs` is raised if needed to cover the longest enabled per-source delay. Buffer sizing is derived from the slowest effective acquisition path (poll period plus delay) and the analysis wait, with a small safety margin. If Redfish is enabled, its heartbeat requirement is included to guarantee coverage. Sanity checks also ensure plausible Redfish cadence and warn if no collectors are enabled. Non-fatal environment hints (for example the RAPL powercap path) are reported at low verbosity.

The result is a single, internally consistent configuration snapshot. Adjustments are announced once at startup to aid reproducibility while avoiding log noise.

#### 1.19.4 Evolution in Newer Kepler Versions

Subsequent Kepler releases (v0.10.0 and later) have replaced the environment-variable system with a unified configuration interface based on CLI flags and YAML files. This modernized approach simplifies configuration management and aligns better with Kubernetes conventions, providing clearer defaults and validation at startup.

Tycho intentionally retains the v0.9.0 model to maintain structural continuity with its experimental foundation. Since configuration handling is not a research focus, adopting the newer scheme would add complexity without scientific benefit. Nevertheless, the newer Kepler design confirms that Tycho's configuration logic can be migrated with minimal effort if long-term maintainability becomes a requirement.

#### 1.19.5 Available Parameters

All parameters are read at startup and remain constant throughout execution. The following table 1.5 summarizes the user-facing configuration variables with their default values and functional scope. Internal or experimental parameters are omitted for clarity.

XX  
CHECK THIS TABLE BEFORE HANDIN, THIS NEEDS CLEANUP  
XX

Variable	Default	Description
<i>Collector enable flags</i>		
TYCHO_COLLECTOR_ENABLE_BPF	true	Enables eBPF-based process metric collection.
TYCHO_COLLECTOR_ENABLE_RAPL	true	Enables RAPL energy counter collection.
TYCHO_COLLECTOR_ENABLE_GPU	true	Enables GPU power telemetry collection.
TYCHO_COLLECTOR_ENABLE_REDISH	true	Enables Redfish-based BMC power collection.
<i>Timing and delays</i>		
TYCHO_TIMEBASE_QUANTUM_MS	1	Base system quantum (ms) defining the global monotonic time grid.
TYCHO_RAPL_POLL_MS	50	RAPL polling interval (ms).
TYCHO_GPU_POLL_MS	200	GPU telemetry polling interval (ms).
TYCHO_REDISH_POLL_MS	1000	Redfish polling interval (ms); should be below BMC publish cadence.
TYCHO_RAPL_DELAY_MS	0	Expected delay between workload change and RAPL visibility (ms).
TYCHO_GPU_DELAY_MS	200	Expected delay between workload change and GPU visibility (ms).
TYCHO_REDISH_DELAY_MS	0	Expected delay between workload change and Redfish visibility (ms).
TYCHO_REDISH_HEARTBEAT_MAX_GAP_MS	3000	Maximum tolerated gap between consecutive Redfish samples (ms).
<i>Autotuning controls</i>		
TYCHO_RAPL_POLL_AUTOTUNE	true	Enables automatic calibration of RAPL polling interval.
TYCHO_RAPL_DELAY_AUTOTUNE	true	Enables automatic calibration of RAPL delay.
TYCHO_GPU_POLL_AUTOTUNE	true	Enables automatic calibration of GPU polling interval.
TYCHO_GPU_DELAY_AUTOTUNE	true	Enables automatic calibration of GPU delay.
TYCHO_REDISH_POLL_AUTOTUNE	true	Enables automatic calibration of Redfish polling interval.
TYCHO_REDISH_DELAY_AUTOTUNE	true	Enables automatic calibration of Redfish delay.
<i>Analysis parameters</i>		
TYCHO_ANALYSIS_TRIGGER	"timer"	Defines analysis trigger: <code>redfish</code> or <code>timer</code> .
TYCHO_ANALYSIS_EVERY_SEC	15	Interval for timer-based analysis (s).
TYCHO_ANALYSIS_DETECT_LONGEST_DELAY	false	Enables detection of the longest observed metric delay.

TABLE 1.5: User-facing configuration variables available in Tycho.

## 1.20 Timing Engine

### 1.20.1 Overview and Motivation

Tycho introduces a dedicated timing engine that replaces the synchronous update loop used in Kepler with an event-driven, per-metric scheduling layer. While the conceptual motivation for this change was discussed in § ??, its practical purpose is straightforward: to decouple the collection frequencies of heterogeneous telemetry sources and to establish a common temporal reference for subsequent analysis.

Each collector in Tycho (e.g., RAPL, eBPF, GPU, Redfish) operates under its own polling interval and is triggered by an aligned ticker maintained by the timing engine. All tickers share a single epoch (base timestamp) and are aligned to a configurable time quantum, ensuring deterministic phase relationships and bounded drift across all metrics. This architecture allows high-frequency sources to capture fine-grained temporal variation while preserving coherence with slower metrics.

The timing engine thus provides the temporal backbone of Tycho: it defines \*when\* each collector produces samples and ensures that all samples can later be correlated on a unified, monotonic timeline. Collected samples are pushed immediately into per-metric ring buffers, described in § 1.21, which retain recent histories for downstream integration and attribution.

### 1.20.2 Architecture and Design

The timing engine is implemented in the `engine.Manager` module. It acts as a lightweight scheduler that governs the execution of all metric collectors through independent, phase-aligned tickers. During initialization, each collector registers its callback function, polling interval, and enable flag with the manager. Once started, the manager creates one aligned ticker per enabled registration and launches each collector in a dedicated goroutine. All tickers share a single epoch, captured at startup, to guarantee deterministic alignment across collectors.

This design contrasts sharply with the global ticker used in Kepler, where a single update loop refreshed all metrics at a fixed interval. In Tycho, each ticker operates at its own cadence, determined by the configured polling period of the respective collector. For instance, RAPL may poll every 50 ms, GPU metrics every 200 ms, and Redfish telemetry every second, yet all remain phase-aligned through the shared epoch.

To maintain temporal consistency, the timing engine relies on the `clock` package, which defines both the aligned ticker and a monotonic timeline abstraction. The aligned ticker computes the initial delay to the next multiple of the polling period and then emits ticks at strictly periodic intervals. Each emitted epoch is converted into Tycho's internal time representation using the `Mono` clock, which maps wall-clock time to discrete quantum indices. The quantum defines the global temporal resolution (default: 1 ms) and guarantees strictly non-decreasing tick values, even under concurrency or system jitter.

The engine imposes minimal constraints on collector behavior: callbacks are expected to perform non-blocking work, typically pushing samples into the respective ring buffer, and to return immediately. This ensures low scheduling jitter and prevents slow collectors from influencing others. Lifecycle control is context-driven: when the execution context is cancelled, all ticker goroutines stop gracefully, and the manager waits for their completion before shutdown.

### 1.20.3 Synchronization and Collector Integration

All collectors in Tycho are synchronized through a shared temporal reference established at engine startup. The `Manager` captures a single epoch and provides it to every aligned ticker, ensuring that all collectors operate on the same epoch even if their polling intervals differ by several orders of magnitude. As a result, each collector's tick sequence can be expressed as a deterministic multiple of the global epoch, allowing later correlation between independently sampled metrics without interpolation artefacts.

Collectors register themselves before the timing engine is started. Each registration includes the collector's name, polling period, enable flag, and a `collect()` callback that executes whenever the corresponding ticker emits a tick. This callback receives both the current execution context and the aligned epoch, which is immediately converted into Tycho's internal monotonic time representation via the `Mono.From()` function. The collector then packages its raw measurements into a typed sample and pushes it to its corresponding ring buffer.

Because all collectors share the same monotonic clock and quantization step, the resulting sample streams can be merged and compared without further time normalization. Fast sources, such as RAPL or eBPF, provide dense sequences of measurements at fine granularity, while slower sources such as Redfish or GPU telemetry produce sparser but phase-aligned data points. This synchronization model eliminates the implicit coupling between sources that existed in Kepler and replaces it with a deterministic, time-driven coordination layer suitable for high-frequency, heterogeneous metrics.

### 1.20.4 Lifecycle and Configuration

The timing engine is initialized during Tycho’s startup phase, after the metric collectors and buffer managers have been constructed. Before activation, each collector registers its collection parameters with the `Manager`, including polling intervals, enable flags, and callback references. Once registration is complete, the engine locks its configuration and starts the aligned tickers. Further modifications are prevented to guarantee a stable scheduling environment during runtime.

At startup, all timing parameters are validated and normalized. Invalid or negative values are rejected or normalized to safe defaults, and the global quantum is verified to be strictly positive. Polling intervals and buffer windows are cross-checked to ensure consistency across collectors, and derived values such as buffer sizes are recomputed from the validated configuration. This guarantees deterministic timing behavior even under partial or malformed configuration files.

The configuration layer also provides flexible control over measurement cadence. Polling periods for individual collectors can be adjusted independently, allowing users to balance temporal precision against system overhead. The default parameters represent a high-frequency but safe baseline: 50 ms for RAPL, 50 ms for eBPF, 200 ms for GPU, and 1 s for Redfish telemetry. All tickers are aligned to the global epoch defined by the monotonic clock, ensuring that these differences in cadence do not lead to drift over time.

Engine termination is context-driven: cancellation of the parent context signals all tickers to stop, after which the manager waits for all goroutines to complete. This unified shutdown mechanism ensures a clean and deterministic teardown sequence without leaving residual workers or buffers in undefined states.

### 1.20.5 Discussion and Limitations

The timing engine establishes the foundation for Tycho’s decoupled and fine-grained metric collection. By aligning all collectors to a shared epoch while allowing individual polling intervals, it eliminates the rigid synchronization that limited Kepler’s temporal accuracy. This design provides a lightweight yet deterministic coordination layer, enabling heterogeneous telemetry sources to contribute time-consistent samples at their native cadence.

The engine’s strengths lie in its simplicity and extensibility. Each collector operates independently, governed by its own aligned ticker, while context-driven lifecycle control ensures deterministic startup and shutdown. Because callbacks perform minimal, non-blocking work, jitter remains bounded even at high polling frequencies. This structure scales naturally with the number of collectors and provides a separation between timing logic, collection routines, and subsequent analysis stages.

Nevertheless, several practical limitations remain. The current implementation assumes a stable system clock and does not compensate for jitter introduced by the Go runtime or external scheduling delays. Collectors are expected to execute quickly; long-running or blocking operations may distort effective sampling intervals. Moreover, the engine’s alignment is restricted to a single node and does not extend to multi-host synchronization, which would require external clock coordination. At

very high sampling rates, the cumulative scheduling overhead may also become non-negligible on resource-constrained systems.

Despite these constraints, the timing engine represents a decisive architectural improvement over Kepler’s fixed-interval model. It provides the temporal backbone for Tycho’s data collection pipeline and enables accurate, high-resolution correlation across diverse telemetry sources. The following section, § 1.21, describes how these samples are buffered and retained for subsequent analysis, completing the temporal layer that underpins Tycho’s measurement and attribution framework.

## 1.21 Ring Buffer Implementation

### 1.21.1 Overview

Tycho employs a per-metric ring buffer to store recent collection ticks produced by the individual collectors. Each collector owns a dedicated buffer that maintains a fixed number of entries, replacing the oldest values once full. This approach provides predictable memory usage and allows fast, allocation-free access to recent measurement histories. All ticks are stored in chronological order and include a monotonic epoch, ensuring consistent temporal alignment with the timing engine. The buffers are primarily used as transient storage for downstream analysis, enabling energy and utilization data to be correlated across metrics without incurring synchronization overhead.

### 1.21.2 Data Model and Sample Types

Each ring buffer is strongly typed and holds a single metric-specific tick structure. These tick types encapsulate all data collected during one polling interval and embed the `SampleMeta` structure, which records Tycho’s monotonic epoch. Depending on the metric, a tick may contain simple scalar values (e.g., total node power) or collections of per-entity deltas (e.g., per-process counters, per-GPU readings, or per-domain energy data). For example, a `RaplTick` stores per-socket energy deltas across all domains, while a `BpfTick` aggregates process-level counters and hardware event deltas observed during that tick. This typed approach simplifies access and ensures that all metric data (regardless of complexity) can be correlated on a uniform temporal axis defined by the timing engine.

### 1.21.3 Dynamic Sizing and Spare Capacity

The capacity of each ring buffer is determined dynamically at startup from the configured buffer window and the polling interval of the corresponding collector. This calculation is performed by the `SizeForWindow()` function, which estimates the number of ticks required to represent the desired time window and adds a small margin of spare capacity to tolerate irregular sampling or short bursts of delayed polls. As a result, each buffer maintains a stable temporal horizon while avoiding premature overwrites during transient load variations. If configuration changes occur, buffers can be resized at runtime, preserving the most recent entries to ensure data continuity across reinitializations.

### 1.21.4 Thread Safety and Integration

Each ring buffer can be wrapped in a synchronized variant to ensure safe concurrent access between collectors and analysis routines. The synchronized type, `Sync[T]`, extends the basic ring with a read-write mutex, allowing simultaneous readers while protecting write operations during tick insertion. In practice, collectors append new ticks concurrently to their respective synchronized buffers, while downstream components such as the analysis engine or exporters read snapshots asynchronously. A central `Manager` maintains references to all buffers, handling creation, resizing, and typed access. This design provides deterministic retention and thread safety without introducing locking overhead into the collectors themselves, keeping the critical path lightweight and predictable.

### 1.21.5 Idle Calibration

logically, idle calibration is part of the analysis portion of tycho.

#### 1.21.5.1 eBPF idle calibration

XX  
CURRENT STATE OF IMPLEMENTATION UNSURE, NEED TO VERIFY XXXXXXXXXXXXXXXXXXXXXXX

#### 1.21.5.2 RAPL idle calibration

XX  
CURRENT STATE OF IMPLEMENTATION UNSURE, NEED TO VERIFY XXXXXXXXXXXXXXXXXXXXXXX

#### 1.21.5.3 GPU idle calibration

XX  
CURRENT STATE OF IMPLEMENTATION UNSURE, NEED TO VERIFY XXXXXXXXXXXXXXXXXXXXXXX

#### 1.21.5.4 redfish idle calibration

XX  
CURRENT STATE OF IMPLEMENTATION UNSURE, NEED TO VERIFY XXXXXXXXXXXXXXXXXXXXXXX

### 1.21.6 Polling frequency Calibration

#### 1.21.6.1 eBPF Polling frequency calibration

Tycho does not perform a dedicated polling-frequency calibration for eBPF-based utilization metrics. eBPF events can be sampled at arbitrarily high rates, and their timing does not depend on hardware update intervals. Instead, Tycho aligns eBPF sampling with the RAPL polling frequency to maintain temporal consistency across collectors. Allowing shorter eBPF intervals would provide limited additional benefit while increasing processing overhead, so eBPF adopts the same lower bound as the CPU energy path and does not require separate calibration.

### 1.21.6.2 RAPL Polling frequency calibration

RAPL updates energy counters at sub-millisecond granularity, but sampling too aggressively introduces noise and diminishes measurement quality. Accuracy is further affected by optional energy filtering mechanisms that reduce fine-grained observability[14, Table 2-2]. Jay et al. found that sampling slower than 50 Hz keeps relative error below 0.5%[15]. Tycho imposes a minimum RAPL polling interval of 50 ms and treats any faster sampling as unnecessary. Because this bound is derived from hardware behaviour rather than runtime variability, Tycho does not include a polling-frequency calibration mechanism for RAPL.

### 1.21.6.3 GPU Polling frequency calibration

Before enabling regular GPU collection, Tycho measures the effective publish cadence of NVML power metrics. Rather than searching over candidate periods, it uses a short *hyperpoll* phase: for the duration of the calibration window, Tycho queries each GPU at a fixed, conservatively fast interval and simply counts how often it sees a new, valid NVML update. From these timestamps it derives inter-arrival gaps and summarises them (via the median) into an estimated publish interval per device.

This converts the problem into “hits over time”: if a GPU produces  $n$  distinct updates over a calibration window of length  $T$ , the observed publish cadence is approximately  $T/n$ , refined by looking at the distribution of individual gaps rather than a single average. Tycho then recommends a per-device polling interval based on this estimate and finally adopts the most conservative (fastest) setting across all GPUs as the node-wide GPU polling period. This approach keeps the implementation simple while ensuring that subsequent GPU collection runs fast enough to see every NVML update without imposing unnecessary overhead.

### 1.21.6.4 Redfish Polling frequency calibration

Redfish power readings are coarse and highly irregular. Publish intervals may vary from sub-second to multi-second gaps, and this variability is further amplified on BMCs that expose multiple chassis or subsystems. Tycho therefore applies a simplified calibration procedure similar to the GPU polling calibration, but adapted to the characteristics of Redfish.

During calibration, Tycho hyperpolls Redfish at the minimum polling interval (500 ms) for a short window (60 seconds). Every newly observed Redfish update (from any chassis exposed by the same BMC) contributes an inter-arrival gap. Using the median of these gaps provides a robust estimate of the typical publish interval while naturally reflecting multi-chassis setups: if one chassis updates faster than others, the calibration converges to that faster cadence, ensuring that no subsystem is undersampled.

Based on this estimate, Tycho selects an operational polling period:

- Without continuous heartbeat, the median publish interval (clamped to 500 ms) is used directly.
- With continuous heartbeat enabled, Tycho selects a smaller polling interval ( $\alpha$  of the median), allowing the collector to detect new samples promptly and maintain accurate freshness tracking despite Redfish’s inherent timing jitter.

This yields a coarse but sufficient estimate of the underlying BMC cadence while relying on the adaptive heartbeat mechanism during normal operation to maintain temporal coherence across all chassis.

### 1.21.7 Delay Calibration

Delay calibration determines the time interval between the start of a workload and the first measurable reaction in the corresponding hardware metric. Because Tycho itself does not execute workloads on the host and does not have direct access to specialised hardware resources, delay calibration must be performed by external scripts that run on the bare-metal node. Each calibration attempt begins with an idle period until the metric reaches a stationary state, followed by a controlled workload with a known start time. The delay is the earliest sample that exceeds the idle baseline by a detectable margin. Since many hardware metrics apply internal averaging or have irregular publish cycles, a single run is not sufficient. Multiple runs are required to obtain a stable distribution. Tycho uses either the minimum or the fifth percentile of observed delays. The minimum reflects the earliest possible reaction. The fifth percentile can be used when the minimum appears to be an outlier.

#### 1.21.7.1 GPU delay calibration

GPU delay calibration uses a dedicated script that generates a controlled GPU workload and monitors NVML power readings. A preliminary attempt relied on `gpu-burn`[16], but this tool carries a non-negligible startup delay that obscures the true hardware reaction time. To address this, the calibration mechanism was reimplemented with Numba[17], which allows the script to launch a custom floating-point kernel with exact control over the workload timing.

The script alternates between idle and active periods. During idle periods, NVML power is sampled until the readings reach a stable baseline, and only the final portion of the idle window is used for statistical analysis. During active periods, the Numba kernel saturates the GPU's compute units while the script continually samples NVML power. The delay is identified as the first sample that exceeds the idle baseline by a small, adaptively computed threshold. Because NVML power reports are averaged over approximately one second, many runs are required to gather a suitable distribution of delays. The default configuration uses 15 seconds of idle time, 15 seconds of active workload, a sampling interval of 50 milliseconds, and 100 runs.

#### 1.21.7.2 RAPL

No dedicated delay calibration is planned for RAPL. With the fast update frequency of RAPL energy counters, access latency is negligible. Although very early work criticised timing characteristics at sub-millisecond resolution[18], later studies generally consider RAPL accurate for the time scales relevant to energy modelling. Tycho enforces a minimum collection interval of 50 milliseconds because RAPL readings are noisy at very short intervals[19]. At this granularity any residual delay is small compared to the sampling window and does not meaningfully affect alignment. Explicit delay calibration would therefore provide minimal benefit.

### 1.21.7.3 Redfish

Redfish presents a fundamentally different problem. Power readings are published slowly, with irregular inter-arrival times, and may skip updates entirely. An earlier empirical study reported delays of roughly 200 milliseconds[20], but also noted substantial variability across systems. Additional indeterminism arises from the network path and the unknown internal behaviour of the BMC. Since Tycho already mitigates staleness through its freshness mechanism, explicit delay calibration is neither feasible nor useful. Redfish is therefore treated as a coarse, low-resolution metric, appropriate for slow global trends but not for fine-grained timing.

### 1.21.7.4 eBPF Metrics

eBPF-based utilisation metrics behave differently. They are collected directly in kernel context and do not involve additional publish intervals or device-side buffering. Their effective delay is negligible relative to Tycho's sampling windows, so no delay calibration is required.

## Chapter 2

# temporary notes on Pijnacker's KUBEWATT

## Summary of Useful Insights from Related Work

### Granularity of Energy Measurement

Most prior work in cloud energy efficiency focuses on cluster-wide or system-wide metrics. Container-level or workload-level energy measurement is largely unexplored. This underscores the need for a fine-grained measurement tool that captures power usage per Kubernetes container.

### Energy-Aware Scheduling

Research on energy-aware schedulers (for example WOA, KIEDS, and Smart-Kube) demonstrates that energy savings between ten and fifteen percent are achievable. All such schedulers rely on node-level energy metrics and cannot address energy waste that originates from individual workloads. They are constrained by the resource requests and limits enforced by Kubernetes. This supports the need for accurate per-container energy measurement as a precursor to optimization.

### Existing Energy Measurement Approaches

Several approaches measure energy in virtualized or containerized systems. Examples include:

- Pod-level energy derived from global node power multiplied by the time a pod is active (coarse approximation).
- SmartWatts, which uses RAPL exclusively but is not applicable in virtualized environments.
- A multi-level power mapping model (bare-metal, virtual machines, Kubernetes) which is promising but not implemented as a usable tool.

Existing tools either lack sufficient validation or lack support for modern production environments. This motivates the creation of a validated Kubernetes-specific measurement system.

## Overprovisioning and Resource Waste

Large-scale studies of cloud resource use show extreme underutilization, with average CPU utilization around ten percent for virtual machines. Techniques for reducing waste (core reduction, shutdown policies) exist but operate at the VM level and conflict with common SLA requirements. These approaches do not address Kubernetes workload-level inefficiencies. This further motivates the need to measure energy use at container level.

## Metrics and Observability

Surveys indicate a lack of consensus on which sustainability metrics should be used. Metrics often combine performance, energy, and emissions components. Tools must be adapted as cloud technologies evolve because some counters are not available on modern systems. Prometheus is identified as the dominant observability stack. Therefore a Kubernetes energy measurement tool should expose metrics in Prometheus format and define a clear and consistent metric set.

## Implications for Tycho and KubeWatt

The related work reinforces several design choices:

- The need to focus on accurate container-level power attribution.
- The use of multiple measurement sources rather than RAPL alone.
- The importance of a structured metric model and Prometheus compatibility.

It also identifies gaps which Tycho and KubeWatt both aim to fill, especially the absence of validated and production-ready tools that target Kubernetes specifically.

## Summary of Useful Insights from Kepler Validation Results

### Single-Stressor CPU Tests

**Inconsistent results between Kepler deployments** The four Kepler deployments (redfish, rapl, default, custom) produce significantly different node power values. The root mean squared error between deployments is very large, with differences of more than 160 W in several cases. Only kepler-default and kepler-custom agree with each other.

**Alignment with external power sources** The kepler-redfish deployment tracks iDRAC total power closely. The kepler-rapl deployment tracks RAPL closely. This indicates that Kepler simply reproduces the external source but does not provide an integrated or corrected view.

**Redfish latency causes attribution artefacts** As iDRAC updates power only once per minute, rapid drops in CPU usage lead to temporary over-attribution of power in Kepler. Kepler distributes the stale node power among running containers, causing artificial power spikes in all namespaces following workload quiescence.

**Incorrect idle-mode power attribution** Kepler attributes idle-mode power to pods that have already completed. In kepler-redfish, idle-mode power per terminated pod is around six watts. In kepler-rapl this is around two and a half watts. In kepler-default and kepler-custom these pods report zero power as expected. This indicates incorrect idle-mode attribution in the non-estimator deployments.

### Container-Level Power Attribution Problems

**Power attributed to non-running containers** Kepler attributes power to completed containers in the idle namespace. This is incorrect and indicates an attribution failure.

**Misattribution to system processes** When many idle pods are deleted simultaneously, power previously attributed to these pods is redistributed as expected. However, dynamic-mode power assigned to the active stressor container decreases, while dynamic-mode power for the system namespace increases. This implies that Kepler misattributes a portion of the stress workload to system-level processes.

**Cause traced to cAdvisor slices** cAdvisor exports CPU usage for real containers as well as for aggregated cgroups and slices (for example kubepods.slice). Kepler does not filter these consistently. This leads to apparent CPU usage that belongs to no namespace and results in misattributed dynamic-mode power. Filtering cAdvisor metrics to actual containers resolves the discrepancy.

### Node Component Tests

**Component-level accuracy depends on RAPL availability** For deployments with RAPL (kepler-rapl and kepler-redfish), the package and DRAM power correspond closely to RAPL component counters. For deployments using estimator models (kepler-default and kepler-custom), component power does not follow the expected patterns and diverges significantly from RAPL. The errors are large: approximately 172 W for package (around 64 percent of max value) and 7 W for DRAM (around 55 percent).

**Estimator models ineffective** Both estimator-based deployments fail to reproduce component power trends. Custom training attempts did not yield usable models. Documentation for training Kepler models is incomplete and inaccurate, making model training impractical.

### Answering the Research Questions

**kpRQ1: Accuracy of node-level measurements** Kepler can closely reproduce its external power sources. However:

- redfish inherits a one-minute update delay which causes significant attribution artefacts,
- RAPL reproduces its own counter values but these counters do not match ground truth server power without calibration,
- estimator models are unusable for accurate node power and deviate by more than 99 percent from ground truth.

**kpRQ2: Accuracy of container-level attribution** Kepler consistently misattributes container energy. Major problems include:

- power assigned to completed pods,
- misattribution to system processes,
- incorrect ratio of idle to dynamic power,
- misalignment caused by redfish latency.

The core attribution model is identical across deployments and therefore all configurations show identical behaviour.

**kpRQ3: Influence of different configurations** Different Kepler configurations drastically change node-level results but do not change container-level attribution behaviour. All deployments share the same attribution model, therefore all share the same attribution errors. Differences in attribution results stem from differences in the underlying node metrics (RAPL, redfish, or estimator).

## Key Insights Relevant for Tycho and KubeWatt

- Node-level accuracy depends entirely on the external power source.
- RAPL cannot be used uncalibrated and diverges from ground truth by a linear relation.
- Redfish latency introduces severe attribution artefacts unless compensated.
- Estimator models in Kepler are unreliable and difficult to train due to poor documentation.
- Container attribution in Kepler is fundamentally incorrect and cannot be fixed by changing the node power source.
- Slice-level CPU usage in cAdvisor must be filtered to avoid misattribution.

This body of findings motivates the creation of a new tool with corrected metric pipelines, usable power models, reliable component attribution, and proper handling of delayed external power sources such as Redfish.

## Summary of Useful Insights from the KubeWatt Architecture

### General Requirements and Design Goals

KubeWatt is introduced as an alternative to Kepler, intended to provide accurate container-level power attribution. Its design requirements are:

1. Read Kubernetes CPU utilization at node and container level.
2. Obtain total node power from some external source.
3. Split node power into static (idle) and dynamic fractions.

4. Export container-level power as Prometheus metrics.

The static power represents the baseline cost of running the node and the Kubernetes control plane. Dynamic power is attributed exclusively to non-control-plane containers.

## Power Split into Static and Dynamic Components

Static power is treated as a constant overhead that does not change over time. Dynamic power is attributed proportionally according to container CPU utilization. All power consumed by the control plane at idle is included in the static value. Additional control plane load that results from workload activity is attributed to the workloads themselves.

## KubeWatt Modes

KubeWatt operates in three modes.

### 1. Base initialization mode

- Assumes an empty cluster running only control plane components.
- User specifies regular expressions identifying control plane pods.
- Measures node power every fifteen seconds for five minutes.
- Computes static power as a simple average.
- Expected to give the most accurate static power value.

### 2. Bootstrap initialization mode

- Designed for clusters with workloads that cannot be shut down.
- Collects node CPU, container CPU and node power every fifteen seconds for thirty minutes.
- Requires a sufficiently varied distribution of CPU usage values.
- Performs bucket analysis to verify that the CPU usage distribution spans a reasonable range.
- Also collects control plane CPU usage to estimate its average idle level.
- Fits a third-degree polynomial to predict node power as a function of CPU load.
- Evaluates the polynomial at the average control plane CPU usage to estimate static power.

**Assumption 1** Static power does not significantly change over time. This assumption is needed because static power is measured once and not updated automatically.

### 3. Estimation mode

This is the main operational mode. It takes the static power and configuration from the initialization phase and produces container-level power attribution metrics.

**Underlying model** KubeWatt adopts a CPU-proportional power mapping model inspired by the pod-mapping concept in Andringa [21]. The original model maps:

- bare-metal power to virtual machine power
- virtual machine power to pod power

based solely on CPU utilization ratios.

**Adapted model for container-level attribution** KubeWatt modifies the model to:

- directly split total node power into static and dynamic parts,
- attribute only dynamic power to containers,
- use the sum of actual container CPU usage as denominator, not node CPU usage from the metrics API.

Equation used:

$$\text{power}(c_{m,i}) = \text{power}_d(n_i) \cdot \frac{\text{cpu}(c_{m,i})}{\sum_j \text{cpu}(c_{j,i})}$$

**Important distinction** The denominator excludes:

- system processes,
- cgroup slices,
- any non-container CPU activity.

These are considered part of static power and must not receive dynamic power attribution.

**Assumption 2** Each Kubernetes node consumes all measurable power of its underlying physical or virtual machine. There are no other workloads outside Kubernetes using power. This assumption is needed to treat the measured node power as node power exclusively.

### Overall Architectural Character

The overall structure of KubeWatt is characterized by:

- a static power estimation step,
- a CPU-proportional dynamic power attribution model,
- reliance on a single power source per node,

- exclusion of system processes and control plane idle consumption from dynamic power,
- export of metrics in Prometheus format.

The model makes strong assumptions about workload exclusivity and static power stability. These assumptions simplify the implementation but may limit applicability in shared or dynamic environments.

## Summary of Useful Insights from the KubeWatt Power and Metrics Collection

### Power Collector

The power collector provides a measurement of node-level power in Watts. KubeWatt defines a PowerCollector interface that abstracts the source of power. The proof-of-concept implementation includes only a Redfish-based collector. Important characteristics:

- Uses the Redfish API exposed by server management interfaces such as iDRAC.
- Each Kubernetes node must be matched to one or more Redfish ComputerSystem entries.
- Host address, user credentials and the list of Redfish systems are supplied by configuration.
- If multiple systems map to a node, their power readings are summed.
- Design is extensible to other sources of power by implementing the interface.

### Kubernetes Metrics Collector

The metrics collector obtains CPU usage for nodes and containers. It uses the following Kubernetes endpoints:

- `metrics.k8s.io/v1beta1/nodes`: node CPU usage in nanoseconds.
- `metrics.k8s.io/v1beta1/pods`: per-container CPU usage in nanoseconds.

The Java Kubernetes client returns pod metrics grouped by namespace. These metrics form the basis for CPU-proportional power attribution.

### Assumptions and Their Consequences

#### Assumption 1: Static power is constant over time

KubeWatt assumes that static (idle) power does not change significantly. This is justified using two months of iDRAC power data from the test server:

- After filtering out active periods, the idle power distribution has a mean of 210.15 W.
- Standard deviation is 0.95 W, which is an error of only 0.45 percent.

- This indicates stable baseline power under the test conditions.

Consequences:

- Static power is measured once and remains fixed.
- If static power drifts slowly over time, KubeWatt will misallocate dynamic power.
- If the machine becomes cooler, actual power may drop below the fixed static value, causing dynamic power to become zero.
- If static power increases, containers will appear to use more dynamic power than they actually do.

### **Assumption 2: Kubernetes is the only workload on the measured machine**

KubeWatt assumes that each node consumes all power measured through Redfish. This is necessary because Redfish only exposes total server power. If external workloads exist, KubeWatt has no information on how to distinguish their power usage.

Consequences:

- KubeWatt cannot operate correctly on shared bare-metal hosts.
- KubeWatt cannot operate correctly on multi-tenant virtual machines unless isolation guarantees hold.
- KubeWatt would misattribute external workload power to Kubernetes containers.

Possible extension (not implemented):

- Use the multi-level mapping model from [21] to distribute bare-metal power across multiple logical partitions such as virtual machines.

## **Overall Architectural Observations**

- The design separates power collection, CPU metrics collection and attribution logic cleanly.
- Only Redfish is supported for power in the prototype.
- The static power assumption simplifies the model but restricts applicability to stable environments.
- KubeWatt does not compensate for Redfish latency and assumes instantaneous node power.
- CPU usage is taken directly from metrics.k8s.io without addressing potential timing skew.
- CPU slices and system processes are excluded by construction, unlike Kepler.

## Summary of KubeWatt Evaluation

### Base Initialization Mode (kwRQ3)

- Base initialization is run on an almost empty cluster (only control plane).
- KubeWatt samples iDRAC power every 15 seconds for 5 minutes and averages it.
- Six repeated runs yield static power values between 198.75 W and 199.15 W.
- The z-scores for these observations are between approximately  $-0.47$  and  $0.31$ .
- Conclusion: base initialization reports static power accurately and consistently.

### Bootstrap Initialization Mode (kwRQ4)

- Bootstrap mode is used when workloads cannot be stopped.
- It collects node CPU, node power and control-plane CPU for 30 minutes (or more) and fits a regression.
- With the initial third-degree polynomial regression and Hyper-Threading enabled:
  - Static power estimates are around 178–185 W, underestimating the base-mode result by 7–11 percent.
  - The accuracy depends strongly on the lower bound of CPU utilization present in the data.
  - When low-CPU data is missing, static power estimates can become grossly inaccurate or even negative.
- The data show a clear knee caused by simultaneous multithreading (SMT).
- Repeating the experiments with SMT disabled yields a nearly linear power versus CPU relation:
  - Linear regression gives  $R^2 \approx 0.94$ .
  - Static power estimates are between 199.9 W and 201.7 W, within 0.4–1.3 percent of the base-mode value.
  - Sensitivity to cuts in the CPU range is much reduced.
- As a result, KubeWatt is changed as follows:
  - Use linear regression instead of a third-degree polynomial.
  - When SMT is enabled, ignore the top 50 percent of CPU utilization data when fitting.
- Conclusion: bootstrap initialization can work well but is inherently less robust and should be second choice after base mode.

## Estimator Mode: Node Power (kwRQ1)

- Estimator mode uses Redfish power and the precomputed static power to infer dynamic power and attribute it to containers.
- In single-stressor tests:
  - Total node power reported by KubeWatt closely follows iDRAC.
  - The root mean squared error of instantaneous power is about 10.56 percent.
  - Most of this error appears when a load just starts, due to delay in Kubernetes CPU metrics.
  - When comparing total energy (area under the curve), the error is below 1 percent.
- This is better than Kepler's best configuration, which showed around 18.7 percent RSME to iDRAC.

## Estimator Mode: Container Attribution (kwRQ2)

### Single-stressor tests

- KubeWatt reports only dynamic power per namespace; static power is exported as a separate quantity.
- Control-plane pods are excluded from dynamic attribution.
- In single-stressor tests, the stress namespace receives dynamic power proportional to its CPU usage, as expected.

### Multi-stressor tests

- Four stressors are run in phases, each using sixteen CPUs, up to full system load.
- KubeWatt attributes equal power to stressor containers that have equal CPU utilization, as expected.
- Power per container decreases once more than 32 threads run simultaneously, which aligns with throughput measurements and the SMT findings.
- cAdvisor does not show this throughput difference since it reports only CPU seconds, not effective work done.

### Transient misattribution during container startup

- When stressor container 0 starts, Redfish power already increases before Kubernetes metrics report CPU usage for that container.
- During this brief window, dynamic power is assigned to containers 1–3 which are idle but visible in the metrics.

- Once all containers are reported by metrics.k8s.io, attribution corrects itself.

### Inactive pod deletion test

- The test with many idle pods that are created and then deleted is repeated for KubeWatt.
- Total system power (iDRAC) is unchanged by deleting idle pods, as expected.
- KubeWatt:
  - does not attribute power to completed idle pods,
  - attributes dynamic power correctly to the stress namespace,
  - keeps the static power term separate.
- Conclusion: KubeWatt does not suffer from the severe attribution problems observed in Kepler. It correctly ignores non-running idle pods and tracks the stressor.

### Overall Evaluation Conclusions

- Base initialization gives accurate and stable static power values.
- Bootstrap initialization is usable but sensitive to workload characteristics and CPU range; it benefits from linear regression and SMT-aware filtering.
- Estimator mode tracks node power well and outperforms Kepler in terms of node-level accuracy relative to iDRAC.
- Container-level dynamic power attribution behaves as intended in both single- and multi-stressor tests and remains stable under creation and deletion of large numbers of idle pods.

## Summary of KubeWatt Discussion and Conclusion

### Discussion of Research Questions

**kwRQ1: Node power accuracy** KubeWatt can read node power accurately from an external source (iDRAC via Redfish). Base and bootstrap initialization both use these readings effectively. In estimator mode, accuracy is good except in short periods where dynamic power is non-zero but no container CPU usage is yet visible in the metrics. In that case, dynamic power cannot be attributed and is temporarily lost.

**kwRQ2: Container power attribution** In general, KubeWatt attributes power to containers in a way that matches CPU utilization, throughput, and the observed power curve. Power is briefly misattributed when new containers start producing load before they appear in the Kubernetes metrics API. Because data is sampled every 15 seconds and metrics are delayed, KubeWatt is only suitable for workloads with relatively stable CPU utilization. KubeWatt only uses CPU as a driver for power, so power usage of GPUs, FPGAs or other accelerators is not represented.

**kwRQ3: Base initialization accuracy** Base initialization reports a very stable static power value with minimal spread (about 0.4 W around a 199 W mean). It is fast (about five minutes) and considered accurate.

**kwRQ4: Bootstrap initialization accuracy** Bootstrap initialization can estimate static power with good accuracy if SMT effects and CPU range are handled correctly. With adjusted regression (linear) and SMT-aware filtering, errors of 0.4–1.3 percent are possible under ideal data, and within about 5 percent for reduced CPU ranges. It remains a second-best option compared to base initialization.

## Overall Conclusion

The main research question asked how to accurately measure or estimate container power from external measurements. Key conclusions:

- Kepler shows serious attribution problems (static power on non-running containers, misattribution to system processes).
- KubeWatt addresses many of these issues by:
  - separating static and dynamic power,
  - excluding control-plane and system processes from dynamic attribution,
  - using a CPU-proportional mapping model,
  - and carefully calibrating static power.
- External metrics have non-negligible latency, which affects both KubeWatt and Kepler and must be considered in any design.
- KubeWatt can provide accurate container power metrics under its assumptions, and in specific tests it outperforms Kepler.
- A key limitation is that KubeWatt considers only CPU as a power driver and therefore cannot handle accelerators such as GPUs or FPGAs.

## Threats to Validity

- Limited Kepler evaluation: only RAPL and Redfish were tested as power sources, not NVML, ACPI or IPMI.
- Hardware issues: the test server had intermittent memory errors, which might influence load and power noise.
- Single-server testbed: no multi-node, multi-workload scenarios; results may not generalize to full datacenter environments.
- Non-ideal environment: the server was located in a warm archival room with fluctuating temperatures rather than a controlled datacenter.
- Synthetic workloads: only stress-ng workloads were used, which may not represent real production workloads.

## Future Work

- Extend KubeWatt with more power collectors and support for accelerators such as GPUs.
- Evaluate KubeWatt on realistic, multi-node Kubernetes workloads.
- Study SMT effects in more detail across different hardware and measurement stacks to explain the observed knee in the power versus CPU curve.

## 1. Improvements KubeWatt Made Over Kepler

### 1.1. Strict Static–Dynamic Power Separation

**Improvement:** KubeWatt explicitly separates total node power into a static (idle) component and a dynamic component. **Addresses Kepler problems:**

- Kepler attributes static/idle power to non-running containers.
- Kepler assigns idle-mode power to completed pods.
- Control-plane idle overhead pollutes workload attribution.

### 1.2. Exclusion of System Processes and Cgroup Slices

**Improvement:** KubeWatt filters out system processes, slice-level aggregates, and non-container cgroups from the CPU denominator. **Addresses Kepler problems:**

- Power assigned to `system_processes`.
- Idle-mode leakage into best-effort slices.

### 1.3. Correct Handling of Control-Plane Workloads

**Improvement:** Idle control-plane CPU is incorporated into the static baseline. **Addresses Kepler problems:** Control-plane activity is distributed across user namespaces.

### 1.4. Robust Static Power Calibration

**Improvement:** Base initialization mode directly measures static power on an empty cluster. **Addresses Kepler problems:** Kepler provides no calibration for static node power.

### 1.5. Statistical Bootstrap Initialization

**Improvement:** When idle windows are unavailable, KubeWatt fits a regression model to CPU–power samples. **Addresses Kepler problems:** No mechanism to infer static power on live, busy clusters.

## 1.6. SMT-Aware Modelling

**Improvement:** KubeWatt detects SMT-induced knees in the CPU–power curve and adjusts regression accordingly. **Addresses Kepler problems:** Kepler assumes linear proportionality even under SMT, causing misattribution.

## 1.7. Transparent Ratio-Based Model

**Improvement:** A simple, explicit CPU-proportional ratio model replaces Kepler’s multi-layered estimator logic. **Addresses Kepler problems:** Undocumented estimator behaviour and inconsistent domain mixing.

## 1.8. Power Collector Abstraction

**Improvement:** Any external power source can be plugged in behind a uniform interface. **Addresses Kepler problems:** Tight coupling between collectors and model code.

## 1.9. Predictable Behaviour under Pod Churn

**Improvement:** The “inactive-pod deletion” test behaves correctly. **Addresses Kepler problems:** Kepler reports power usage for terminated pods.

## 1.10. Deterministic, Low-Latency Metric Ingestion

**Improvement:** KubeWatt relies solely on the metrics-server pipeline, making delay behaviour predictable. **Addresses Kepler problems:** Mixed eBPF, cAdvisor, and API sources yield inconsistent timing and alignment.

# 2. Implementation Elements Tycho Should Adopt

## 2.1. High-Impact Features

1. **Static–Dynamic Power Separation.** Tycho should follow KubeWatt’s approach of subtracting static power prior to container attribution.
2. **Strict Cgroup Filtering.** Tycho should exclude / ignore slice-level cgroups and system processes when summing container CPU.
3. **Explicit Control-Plane Handling.** Idle control-plane CPU should be treated as static; additional usage should be attributed to workloads indirectly causing it.
4. **Dedicated Baseline Calibration Module.** Adopt both base-mode calibration and a bootstrap fallback.
5. **SMT-Aware Resource Modelling.** Tycho should incorporate SMT-aware filtering or data selection to avoid non-linear artefacts.
6. **Pluggable Power Collector Architecture.** Ensure clean separation between collectors such as RAPL, Redfish, NVML, BMC-derived metrics, etc.

7. **Transparent Ratio Model.** Retain the simple proportional model

$$\text{power}(c) = \text{power}_d(n) \cdot \frac{\text{cpu}(c)}{\sum \text{cpu}(c)},$$

as a well-understood baseline.

## 2.2. Medium-Impact Features

- Bootstrap-mode estimation for static power when idle windows do not occur.
- Incorporation of metric-latency handling using Tycho's timing engine.
- Explicit omission of static power from per-container metrics.

## 2.3. Low-Impact Features

- User-configurable control-plane pod matching (e.g. via regex).
- Linear-regression fallback in calibration when SMT is disabled.

# 3. Overall Assessment of KubeWatt

## 3.1. Strengths

- Conceptually simple and transparent architecture.
- Fixes several fundamental attribution errors present in Kepler.
- Provides robust static power calibration mechanisms.
- Achieves very close correspondence to ground-truth node power.
- Handles churn and multi-stressor workloads more reliably than Kepler.

## 3.2. Weaknesses

- CPU-only; ignores GPU, FPGA, NVMe, and domain-level energy.
- Assumes Kubernetes is the sole workload on a machine.
- Depends on the metrics-server pipeline with coarse temporal granularity.
- Assumes static power remains constant over long time scales.
- No timing alignment or latency correction compared to Tycho's design.

## 3.3. Summary

KubeWatt represents a clean, pragmatic rethinking of container-level energy attribution. It addresses many of Kepler's correctness issues through careful separation of static and dynamic power, strict CPU accounting, and explicit calibration. However, its scope is intentionally narrow: it is CPU-only, single-tenant, and limited by

the latency of the Kubernetes metrics pipeline. In contrast, Tycho aims for higher accuracy, multi-source integration, timing alignment, and support for accelerated workloads. Nonetheless, several design principles from KubeWatt should directly inform Tycho's implementation.

# Bibliography

- [1] Caspar Wackerle. *PowerStack: Automated Kubernetes Deployment for Energy Efficiency Analysis*. GitHub repository. 2025. URL: <https://github.com/casparwackerle/PowerStack>.
- [2] International Energy Agency. *Energy and AI*. Licence: CC BY 4.0. Paris, 2025. URL: <https://www.iea.org/reports/energy-and-ai>.
- [3] Ryan Smith. *Intel's CEO Says Moore's Law Is Slowing to a Three-Year Cadence — But It's Not Dead Yet*. Accessed: 2025-04-14. 2023. URL: <https://www.tomshardware.com/tech-industry/seminconductors/intels-ceo-says-moores-law-is-slowing-to-a-three-year-cadence-but-its-not-dead-yet>.
- [4] Martin Keegan. *The End of Dennard Scaling*. Accessed: 2025-04-14. 2013. URL: <https://cartesianproduct.wordpress.com/2013/04/15/the-end-of-dennard-scaling/>.
- [5] Uptime Institute. *Global PUEs – Are They Going Anywhere?* Accessed: 2025-04-14. 2023. URL: <https://journal.uptimeinstitute.com/global-pues-are-they-going-anywhere/>.
- [6] Eric Masanet et al. "Recalibrating global data center energy-use estimates". In: *Science* 367.6481 (2020), pp. 984–986. doi: 10.1126/science.aba3758. eprint: <https://www.science.org/doi/pdf/10.1126/science.aba3758>. URL: <https://www.science.org/doi/abs/10.1126/science.aba3758>.
- [7] Amit M. Potdar et al. "Performance Evaluation of Docker Container and Virtual Machine". In: *Procedia Computer Science* 171 (2020), pp. 1419–1428. issn: 1877-0509. doi: 10.1016/j.procs.2020.04.152.
- [8] Roberto Morabito. "Power Consumption of Virtualization Technologies: An Empirical Investigation". In: *2015 IEEE/ACM 8th International Conference on Utility and Cloud Computing (UCC)*, Dec. 2015, pp. 522–527. doi: 10.1109/UCC.2015.93. (Visited on 05/21/2025).
- [9] Linux Foundation Energy and Performance Working Group. *Kepler: Kubernetes-based Power and Energy Estimation Framework*. Accessed: 2025-11-14. 2025. URL: <https://github.com/sustainable-computing-io/kepler>.
- [10] Hubblo. *Scaphandre: Energy consumption monitoring agent*. <https://github.com/hubblo-org/scaphandre>. Accessed: 2025-06-24. 2025.
- [11] Caspar Wackerle. *Tycho: an accuracy-first container-level energy consumption exporter for Kubernetes (based on Kepler v0.9)*. GitHub repository. 2025. URL: <https://github.com/casparwackerle/tycho-energy>.
- [12] NVIDIA Corporation. *NVML API Reference Guide*. Function `nvmlDeviceGetPowerUsage`: retrieves GPU power usage in milliwatts. 2024. URL: [https://docs.nvidia.com/deploy/pdf/NVML\\_API\\_Reference\\_Guide.pdf](https://docs.nvidia.com/deploy/pdf/NVML_API_Reference_Guide.pdf) (visited on 11/13/2025).
- [13] Yole Group. *Data Center Semiconductor Trends 2025: Artificial Intelligence Reshapes Compute and Memory Markets*. Press Release. 2025. URL: <https://www.yolegroup.com/press-release/data-center-semiconductor-trends-2025-artificial-intelligence-reshapes-compute-and-memory-markets/>.
- [14] Intel Corporation. *Intel® 64 and IA-32 Architectures Software Developer's Manual Volume 4: Model-Specific Registers*. Tech. rep. 335592-081US. Accessed 2025-04-28. Intel Corporation, Sept. 2023. URL: <https://cdrdv2.intel.com/v1/dl/getContent/671098>.
- [15] Mathilde Jay et al. "An Experimental Comparison of Software-Based Power Meters: Focus on CPU and GPU". In: *2023 IEEE/ACM 23rd International Symposium on Cluster, Cloud and Internet Computing (CCGrid)*, May 2023, pp. 106–118. doi: 10.1109/CCGrid57682.2023.00020. (Visited on 04/21/2025).
- [16] wilicc. *gpu-burn: Multi-GPU CUDA stress test*. <https://github.com/wilicc/gpu-burn>. Accessed: 2025-11-18. 2025.
- [17] The Numba Developers. *Numba: A High Performance Python Compiler*. <https://numba.pydata.org/>. Accessed: 2025-11-18. 2025.
- [18] Kashif Nizam Khan et al. "RAPL in Action: Experiences in Using RAPL for Power Measurements". In: *ACM Trans. Model. Perform. Comput. Syst.* 3.2 (Mar. 2018), 9:1–9:26. issn: 2376-3639. doi: 10.1145/3177754. (Visited on 04/07/2025).
- [19] Robert Schöne et al. "Energy Efficiency Features of the Intel Alder Lake Architecture". In: *Proceedings of the 15th ACM/SPEC International Conference on Performance Engineering*, London United Kingdom: ACM, May 2024, pp. 95–106. ISBN: 979-8-4007-0444-4. doi: 10.1145/3629526.3645040. (Visited on 04/07/2025).
- [20] Yewan Wang et al. "An Empirical Study of Power Characterization Approaches for Servers". In: *ENERGY 2019 - The Ninth International Conference on Smart Grids, Green Communications and IT Energy-aware Technologies*, June 2019, p. 1. (Visited on 04/23/2025).